Fossil Record 29 (1) 2026, 185–210 | DOI 10.3897/fr.29.185733

PENSOFT

für Natur MUSEUM FÜR NATURKUNDE BERLIN

A well-preserved specimen of *Stenopterygius quadriscissus* (Reptilia, Ichthyosauria) from the Early Jurassic (Toarcian) of Yorkshire, UK and new insights into species delineation in the genus

Timothée Biot[1,2], Dean R. Lomax[3,4], Feiko Miedema[5], Erin E. Maxwell[2]

1 *Département Sciences de la Terre, University of Lille, Cité Scientifique, Bât. SN5, Avenue Paul Langevin - 59655 Villeneuve d'Ascq Cedex, France*
2 *Staatliches Museum für Naturkunde Stuttgart, Rosenstein 1, 70191 Stuttgart, Germany*
3 *Palaeobiology Research Group, School of Earth Sciences, University of Bristol, Bristol, UK*
4 *Department of Earth and Environmental Sciences, The University of Manchester, Manchester, UK*
5 *Naturhistoriskmuseum, Universitetet i Oslo, Kabelgaten 40, 0581 Oslo, Norway*

https://zoobank.org/ECA6AD31-3060-4FB4-9BEC-A1437C3DA07F

Corresponding author: Erin E. Maxwell (erin.maxwell@smns-bw.de)

Academic editor: Florian Witzmann ♦ **Received** 20 January 2026 ♦ **Accepted** 21 April 2026 ♦ **Published** 8 May 2026

Abstract

Despite abundant and productive Toarcian ichthyosaur-bearing localities in continental Europe, in the UK, Toarcian ichthyosaurs may often be fragmentary and/or too poorly preserved for positive identification. Here, we describe a nearly complete ichthyosaur from the Toarcian (Lower Jurassic) Whitby Mudstone Formation at Ravenscar near Whitby, Yorkshire, England. Preliminary identification supported referral to the genus *Stenopterygius*; however, the hind limb and girdle were not preserved, creating difficulties for species determination. To better undertake comparisons, we revised Toarcian species of the genus *Stenopterygius*, resulting in the recognition of *S. longipes* as a senior synonym of *S. uniter* and *Magnipterygius huenei* as a junior synonym of *S. quadriscissus*. We also identified new metrics pertaining to the caudal skeleton and proximal fore-limb that appear useful for differentiating species when the skull and/or hind-limb is missing or damaged and, thus, applicable to a much greater number of specimens. The Ravenscar specimen is consistent with *S. quadriscissus* and represents one of the youngest stratigraphic occurrences of that species and the first definitively confirmed from the Toarcian of Yorkshire and probably the UK. Our revision resulted in a re-appraisal of species-level diversity in *Stenopterygius* in the Cleveland Basin and throughout the European Toarcian epicontinental basins, with many of the specimens previously identified as *S. triscissus* now confidently attributable to *S. quadriscissus*. These results will facilitate a detailed understanding of vertebrate palaeobiogeography and habitat use in well-studied Jurassic epicontinental basins.

Key Words

Ichthyosauria, Jurassic, morphology, Posidonienschiefer Formation, *Stenopterygius*, taxonomy, Toarcian, Whitby Mudstone Formation

Introduction

Ichthyosaurs are a group of secondarily adapted Mesozoic marine diapsid reptiles with an often dolphin-like body shape. Appearing shortly after the end-Permian extinction (Kear et al. 2023), they rapidly evolved specialisations for life in a pelagic habitat, including large eyes, streamlined bodies and modification of the limbs into flippers, becoming important upper trophic level consumers in the Mesozoic seas prior to their extinction at the Cenomanian-Turonian boundary (Bardet 1992; Motani 2005; Sander et al. 2021; Roberts et al. 2025). Despite their long stratigraphic range, only a few localities globally produce abundant articulated ichthyosaurian skeletons. During the Early Jurassic, the most productive and best known of these include the Blue Lias and Charmouth Mudstone Formations in England (Sharpe 2024), as well the Posidonienschiefer

Formation (Toarcian, Germany), which has yielded thousands of specimens (Sander 2000).

Despite abundant and productive Toarcian ichthyosaur-bearing localities in continental Europe (reviewed by Fischer et al. (2011); Martin et al. (2021); Klug et al. (2024)), in the UK the published record of associated Toarcian ichthyosaur remains is sparse, leading to the impression that these are either uncommon to rare and/or poorly preserved. Ichthyosaurs have been documented from the Whitby region in Yorkshire (Benton and Spencer 1995; Lomax 2019), Strawberry Bank, Somerset (Williams et al. 2015; Srdic et al. 2021) and Rutland (Larkin et al. 2023) (Fig. 1A). Three genera (*Eurhinosaurus*, *Temnodontosaurus*, *Stenopterygius*; Lomax (2019); Weedon and Chapman (2022)) are known from the Toarcian of the Yorkshire area, the majority being found along the Whitby coastline. Most of these specimens are historical and/or fragmentary and often poorly preserved or poorly prepared, leading to difficulties in correctly assessing their taxonomic position (Benton and Taylor 1984; Lomax and Gibson 2015; Lomax 2019). Moreover, the high intraspecific variability present in some genera of Early Jurassic ichthyosaurs, such as *Stenopterygius*, has led to numerous revisions of their systematics over the last three decades (Godefroit 1994; McGowan and Motani 2003; Maisch 2008; Maxwell 2012; Maisch and Matzke 2022). Material referred to genus or species using older diagnostic criteria requires revision, as it may be indeterminate by modern standards. This task is non-trivial: a basic understanding of ichthyosaurian generic and species distribution in the Toarcian has the potential to shed light on potential environmental factors affecting distribution and abundance in these well-studied Jurassic marine reptiles (e.g. Maisch and Ansorge (2004); Zverkov et al. (2020)).

Taxonomic practice in the genus *Stenopterygius* has changed considerably through time. Around the beginning of the 21st century, Toarcian ichthyosaurs referred to *Stenopterygius* were diagnosed by intracranial ratios (snout ratio, orbital ratio, premaxillary ratio, maxillary ratio: Godefroit (1994); McGowan and Motani (2003)), dentition, body size, ratio of limb lengths and vertebral counts. Eight species were recognised as valid (McGowan and Motani 2003). In 2008, Maisch revised the genus, reducing the number of valid species to three (*S. quadriscissus*, *S. triscissus* and *S. uniter*) and re-assigning some material previously referred to *Stenopterygius* to a new genus, *Hauffiopteryx* Maisch, 2008. To differentiate species of *Stenopterygius*, intracranial ratios, dentition, skull size, length of fore-limbs and body shape were still emphasised. However, Maisch (2008) was unable to refer juveniles to species using these metrics since, depending on allometric growth, ratio values varied over ontogeny. He therefore determined all names established, based on small individuals to be nomina dubia (Maisch 2008). Maxwell (2012) conducted new bivariate and multivariate metrics capable of determining species across all ontogenetic stages: *Stenopterygius quadriscissus* was differentiated from the other two species across all body sizes by a relatively longer femur and ischiopubis when compared to lower jaw length, whereas the premaxilla and lower jaw were proportionately longer relative to the femur and ischiopubis in *S. triscissus*. *Stenopterygius uniter* (= *S. longipes* herein) was characterised by elongate fore-limbs relative to the humerus and a shorter femur than in *S. quadriscissus* relative to the length of the lower jaw and also relative to the hind-limb. Unfortunately, the importance of the pelvic girdle and hind-limb, articulated limbs and complete, undamaged jaws required for species determination using these metrics limited the pool of specimens to which this method could be applied. Thus, referral of small specimens for which the hind-limb is lacking remains problematic in this genus. Most recently, Maisch and Matzke (2022) erected a new genus of Early Jurassic ichthyosaur, *Magnipterygius*, based on cranial characters and caudal ratios. Despite many comparisons with *S. triscissus*, none was undertaken with *S. quadriscissus* and an in-depth comparison with juveniles of the latter species is still required.

Here, we describe one of the most complete and well-preserved publicly accessible ichthyosaurs from the Toarcian of Yorkshire (SMNS 55110). Although excavated in 1981, this specimen has not previously been described and was recently examined by one of us (DRL), who determined its local significance (to Yorkshire), which led to this study and a critical evaluation of its taxonomic position. Preliminary observation suggested that this specimen showed similarities to *Stenopterygius*, best known from the Posidonienschiefer Formation of south-western Germany. However, the hind-limb and girdle are not preserved, creating difficulties for species determination. To better undertake comparisons with SMNS 55110, we identify some promising new metrics potentially useful for differentiating species of *Stenopterygius* when the skull and/or hind-limb is missing or damaged and, thus, applicable to a much greater number of specimens. Our revision results in a re-appraisal of species-level diversity in *Stenopterygius* in the Cleveland Basin and throughout the European Toarcian epicontinental basins.

Geology

The Whitby Mudstone Formation is dominated by a commonly laminated dark-grey mudstone (Simms 2004). This formation is divided into five members: the Grey Shale, Mulgrave Shale, Alum Shale, Peak Mudstone and Fox Cliff Siltstone (Fig. 1B). The Whitby Mudstone Formation exposes a total thickness of about 120 metres on the Yorkshire coast, comprising all substages of the Lower Toarcian and some of the Upper Toarcian (Tenuicostatum – Variabilis Zones). The depositional environment during the Early Toarcian is characterised as an epicontinental sea deposited during a marine transgression (Hesselbo and Jenkyns 1999; Hesselbo 2008). Water depths in the Cleveland Basin are estimated to

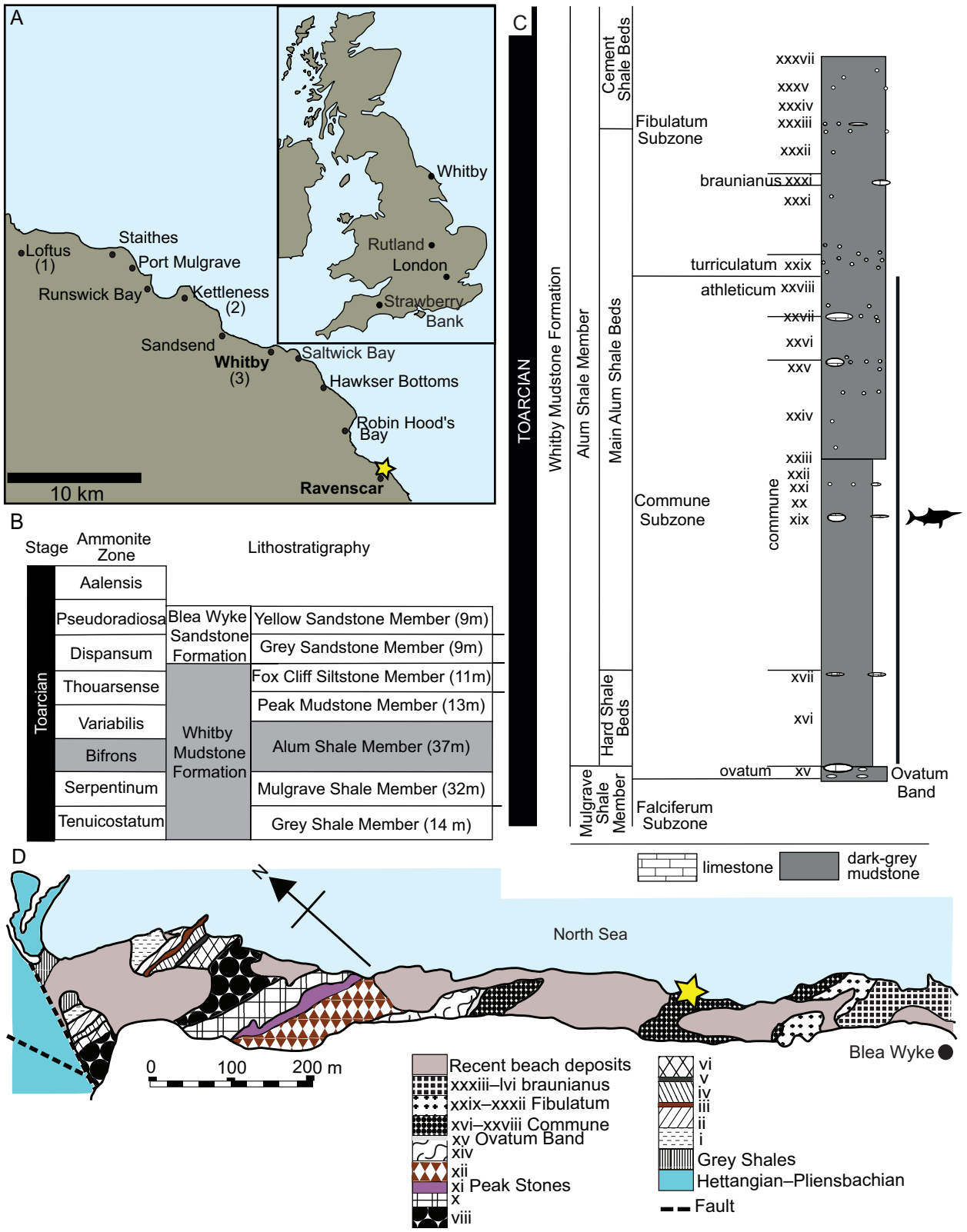

Figure 1. Collection locality of SMNS 55110. **A.** Fossil localities around Whitby, with the locality of SMNS 55110 indicated by a star. The inset indicates position of Whitby relative to other UK Toarcian localities (modified from Swaby and Lomax 2021; 1 = type locality of *Temnodontosaurus zetlandicus*; 2 = type locality of *T. crassimanus*; 3 = approximate type locality of *Eurhinosaurus longirostris*); **B.** Chronostratigraphic correlation of the Whitby Mudstone Formation (modified from Simms 2004); **C.** Stratigraphy of the Mulgrave Shale and Alum Shale Members of the Whitby Mudstone Formation (modified from Simms (2004), with bed numbers corresponding to those of Howarth (1962)); stratigraphic position of SMNS 55110, based on belemnites indicated by silhouette from PhyloPic (*Stenopterygius quadriscissus*, public domain); **D.** Map of the Whitby Mudstone Formation at Ravenscar between Peak Fault and Blea Wyke. Yellow star = documented collection locality of SMNS 55110. Modified from Howarth (1962).

have been > 30 m, up to 100 m during the deposition of the Bifrons Zone (Hallam 1997; Jarvis et al. 2024).

The Toarcian deposits are correlated with the Toarcian Oceanic Anoxic Event (TOAE) leading to the deposition of laminated black shales due to a prolonged period of warming and sea floor anoxia that have favoured the preservation of marine fossils (Martill 1993; Martin et al. 2021). The TOAE has been recognised as one of the main hyperthermal events of the Phanerozoic; this event is associated with the release of a large amount of isotopically light carbon (Hesselbo et al. 2007; Kemp et al. 2022) and with a sea-level rise exceeding 50 metres (Krencker et al. 2019). The release of such amounts of carbon led to seawater temperature increases of up to 7 °C (Rosales et al. 2004; Suan et al. 2008).

Institutional abbreviations

BRLSI, Bath Royal Literary and Scientific Institution, Bath, UK; **GPIT**, Palaeontological Collection of Tübingen University, Tübingen, Germany; **NHMUK**, Natural History Museum, London, UK; **NMBE**, Naturhistorisches Museum Bern, Bern, Switzerland; **NMNHL**, National Museum of Natural History Luxembourg, Luxembourg, Luxembourg; **SMNS**, Staatliches Museum für Naturkunde Stuttgart, Stuttgart, Germany; **WHITM**, Whitby Museum, Whitby, UK; **ZIN PH**, Paleoherpetological Collection, Zoological Institute of the Russian Academy of Sciences, Saint Petersburg, Russia.

Materials and methods

SMNS 55110 was collected in 1981 by Swiss collector Urs Oberli and prepared from its stratigraphically upper surface. The specimen originated from the Whitby Mudstone Formation, North Yorkshire (Fig. 1), from between Peak Fault and Blea Wyke, Ravenscar, in the Alum Shale Member of the Whitby coastline (Fig. 1C; Bifrons Zone, lower Toarcian, Lower Jurassic: Howarth (1962); Simms (2004)). The documented locality represents the Commune Subzone (Howarth (1962): pl. 27; beds 49–59); belemnites (*Acrocoelites* (*Odontobelus*) *vulgaris*, *Acrocoelites* (*Acrocoelites*) *subtenuis* and *Simpsonibelus dorsalis*) associated with the ichthyosaur are consistent with this determination (P. Doyle, pers. comm. (2026)) (Fig. 1D). Multiple individuals of the epifaunal bivalve *Meleagrinella*, ranging in size from 5 to 10 mm in diameter are concentrated towards the top of the skeleton, suggesting that deposition occurred during a relatively short oxic to dysoxic period (Caswell et al. 2009).

Photogrammetric models of SMNS 55110 and SMNS 96922 (holotype of *Magnipterygius huenei*) were produced to increase specimen accessibility. The model of SMNS 55110 was generated from 89 photos taken with a Canon EOS 200D DSLR. The model of SMNS 96922 was constructed from 53 photographs using the same camera. The photos were aligned in Agisoft Metashape (professional licence, v. 2.1.0), which was also used to create a 3D model point cloud and create the mesh, then Meshlab (version: 2022.02) was used to align, clean, scale and orientate the 3D model. Lastly, we used Paraview (version: 4.1.0) to create the depthmap of the model, using gist_earth, a colour vision deficiency-accessible palette. Both photogrammetric models are archived on Morphosource (Media ID 000771213, 000771193).

Species differentiation

Three postcranial metrics were explored as potentially useful for differentiating species in *Stenopterygius*: relative lengths of the pre- and postflexural caudal skeleton (Maisch and Matzke 2022), lengths of the radial and ulnar facets of the intermedium and the angle between these facets.

Caudal measurements were taken from 40 specimens of *Stenopterygius* from the Posidonienschiefer Formation, southwest Germany (Tenuicostatum to Bifrons Zones) assigned to species using independent criteria (Maisch 2008; Maxwell 2012): 29 identified as *Stenopterygius quadriscissus*, seven identified as *Stenopterygius triscissus* and four identified as *Stenopterygius longipes* (see below for taxonomic remarks). Seven of these specimens were juveniles. SMNS 55110 and SMNS 96922 (*Magnipterygius huenei* holotype: Maisch and Matzke (2022)) were also included. The position of the first caudal centrum was determined by the presence of a synapophysis and the relative length of the ribs (McGowan and Motani 2003). Caudal measurements including tailstock length (sensu Buchholtz (2001); = postsacral-preflexural length) and postflexural length (Fig. 2A) were taken by measuring the length of vertebral segments approximating straight lines. Lengths of disarticulated centra were also measured and added to the total. Total caudal length is equal to the sum of postflexural and tailstock length.

Intermedium measurements (Fig. 2C) were assessed, based on 35 of the 40 specimens for which caudal measurements were taken (excluding SMNS 55933, SMNS 80062, SMNS 54819, GPIT-PV-30040 and SMNS 12821 due to poor preservation of the fore-limbs); 11 additional specimens were added as they presented well preserved fore-limbs, but not a well preserved tail (2 *S. triscissus*: SMNS 50007, GPIT-PV-30054; 7 *S. quadriscissus*: SMNS 80115, SMNS 54026, SMNS 51154, SMNS 53001, GPIT-PV-30018, GPIT-PV-30033, GPIT-PV-30060; and 2 *S. longipes*: SMNS 81719, GPIT-PV-30032).

All measurements were taken digitally in the software Inkscape and Gimp. All photos used for the measurements were taken using a Canon EOS 200D DSLR. Most of specimens were studied first-hand, but some were measured from literature. Measurements were taken three times by the first author and the mean value was recorded. Linear regressions and boxplots were realised with the software Rstudio (version 2024.12.0+467).

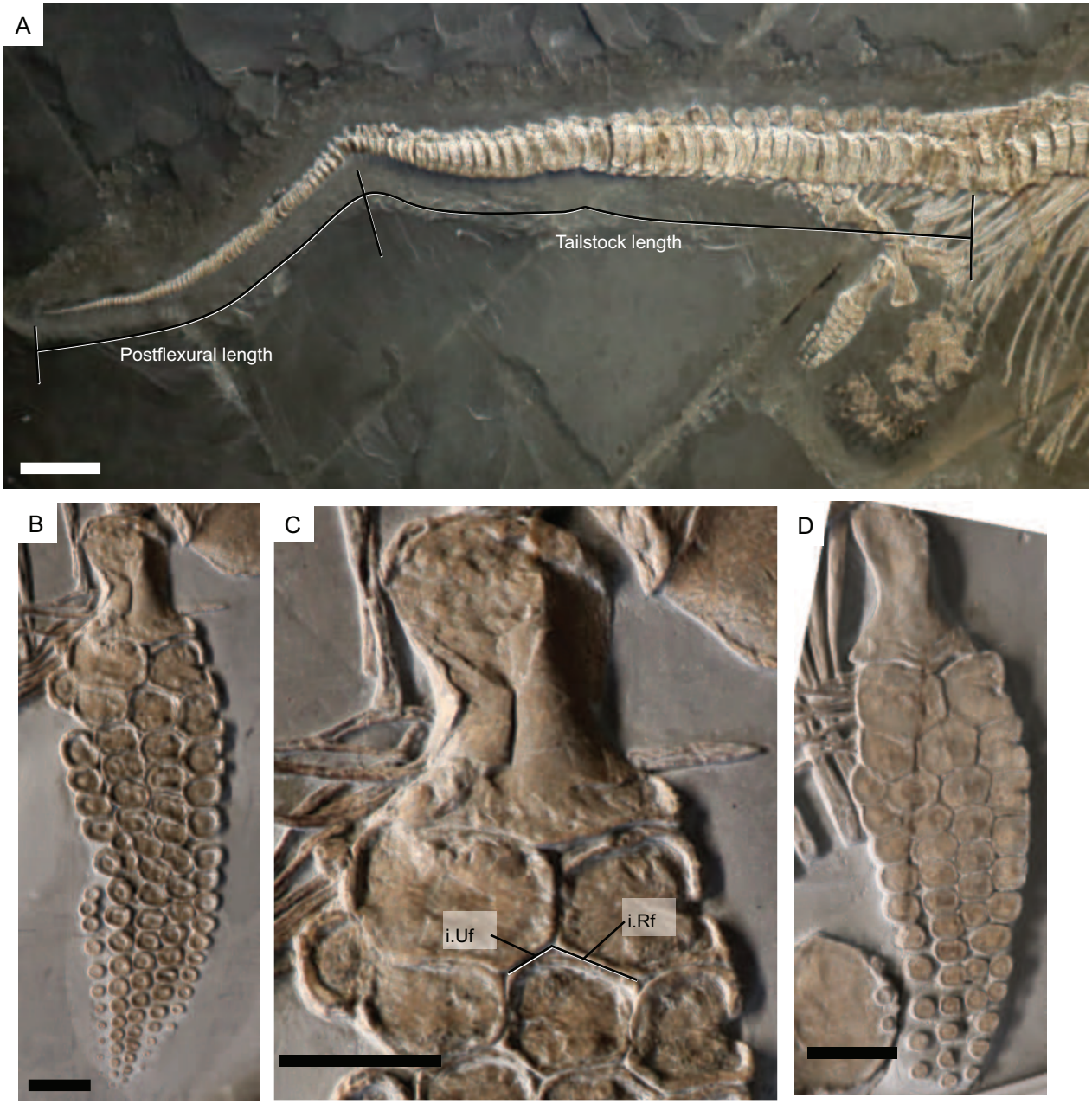

Figure 2. Caudal and fore-limb measurements used to differentiate *Stenopterygius* species. **A.** Tailstock and postflexural caudal measurements (SMNS 56584); **B.** *S. quadriscissus* fore-limb and close-up of the intermedium (GPIT-PV-30051) (**C**), illustrating the radial and ulnar facet measurements; **D.** *S. triscissus* fore-limb (GPIT-PV-30054), illustrating differences in radial and ulnar facet lengths. Abbreviations: i.RF, radial facet of the intermedium; i.UF, ulnar facet of the intermedium. Scale bar equals 10 cm (**A**); 5 cm (**B–D**).

Results

Species differentiation in *Stenopterygius*

A linear regression of postflexural length to total caudal length was undertaken (Fig. 3A, B). Although log transformation of these data reduced variance at larger body sizes (Fig. 3B), both transformed and untransformed data are presented to facilitate comparisons with ratio and count data. These variables scaled isometrically when log-transformed for both taxa, but differed in the intercept, indicating that the postflexural region made up a greater proportion of the tail over all body sizes in *S. quadriscissus* relative to *S. triscissus*. When not transformed, the slope of this relationship differed between the species. *S. quadriscissus* has a postflexural length/total caudal length ratio of 0.39 (+/- 0.032), while *S. triscissus* has a ratio of 0.34 (+/- 0.021) (Fig. 3C). The lowest ratio values obtained from *S. quadriscissus* (0.34; Fig. 3C) pertained to juvenile specimens. Tailstock vertebral counts differed between the two species, with *S. quadriscissus* having a mean count of 35.6 (+/- 2.45) tailstock vertebrae, while *S. triscissus* had 39.8 (+/- 3.13) (Fig. 3D). *Stenopterygius longipes* exhibited a similar range to that of *S. quadriscissus* (35–38 tailstock vertebrae), although sample size was quite small (n = 3). The postflexural region comprises a greater proportion of the total caudal length in

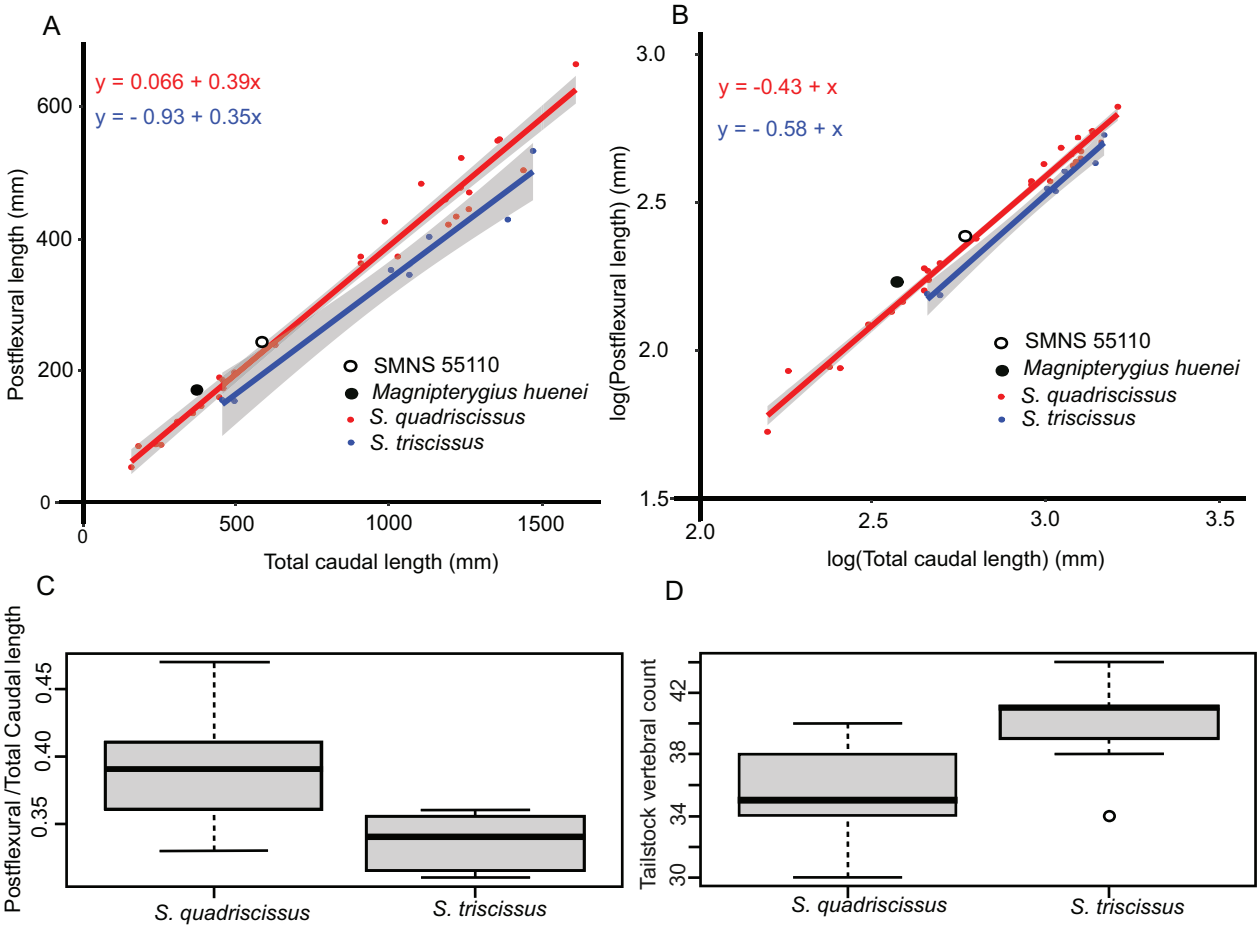

Figure 3. Caudal measurements used to differentiate *Stenopterygius quadriscissus* (n = 29) and *S. triscissus* (n = 7). **A, B.** Linear regression of postflexural length/Total caudal length (mm); SMNS 55110 (Ravenscar ichthyosaur) and SMNS 96922 (holotype of *Magnipterygius huenei*) plotted for reference. **A.** Untransformed data; **B.** Log transformed data; shaded areas represent the 95% confidence interval of the slope. **C.** Boxplot of the postflexural length/Total caudal length ratio; **D.** Boxplot of the tailstock vertebral count in *S. quadriscissus* and *S. triscissus*.

S. quadriscissus than in *Stenopterygius triscissus* and this difference is attributed to a reduced number of tailstock vertebrae in *S. quadriscissus*.

The intermedium measurements were also able to differentiate *S. quadriscissus* and *S. triscissus*. The angle formed by the intermedium, radius and ulna in the proximal fore-limb showed slight differences between the species (Fig. 3D). The mean value for *S. quadriscissus* was equal to 113.4° (+/- 7.3°), while the mean value in *S. triscissus* was slightly more obtuse at 119.5° (+/- 5.2°). However, high intraspecific variation made it difficult to distinguish species with this character alone.

The length of the ulnar facet/length of the radial facet of the intermedium, Uf/Rf, as a character permitted clear separation of the three species, unlike the other metrics that did not differentiate *S. longipes* from the other taxa. The linear regression data showed higher variance (lower r^2) than the vertebral data and, if not log-transformed, converged at smaller body sizes (Fig. 4A). Log transformation to equalise variance at larger body size indicated that this relationship scaled nearly isometrically across taxa (Fig. 4B). Ratio data indicate that there is a proportionately longer contact between the radius and the intermedium than the ulna and intermedium in *S. quadriscissus* (Uf/Rf = 0.84 +/-0.14), while in the two other species, the contact between the intermedium and the ulna is larger (*S. triscissus*: Uf/Rf = 1.36 +/- 0.19; *S. longipes*: Uf/Rf = 1.09 +/- 0.06) (Fig. 4C). Only two specimens of *S. quadriscissus* overlap the range of *S. longipes* and do not overlap *S. triscissus*.

In summary, while these three variables sufficed to differentiate *S. quadriscissus* from *S. triscissus*, the results were not conclusive (except for one measurement pair) for *S. longipes*. This is mainly due to the low number of relatively complete available specimens of *S. longipes*.

Systematic Palaeontology

Ichthyosauria de Blainville, 1835
Parvipelvia Motani, 1999

Genus Stenopterygius Jaekel, 1904

Type species. *Stenopterygius quadriscissus* (Quenstedt, 1856).

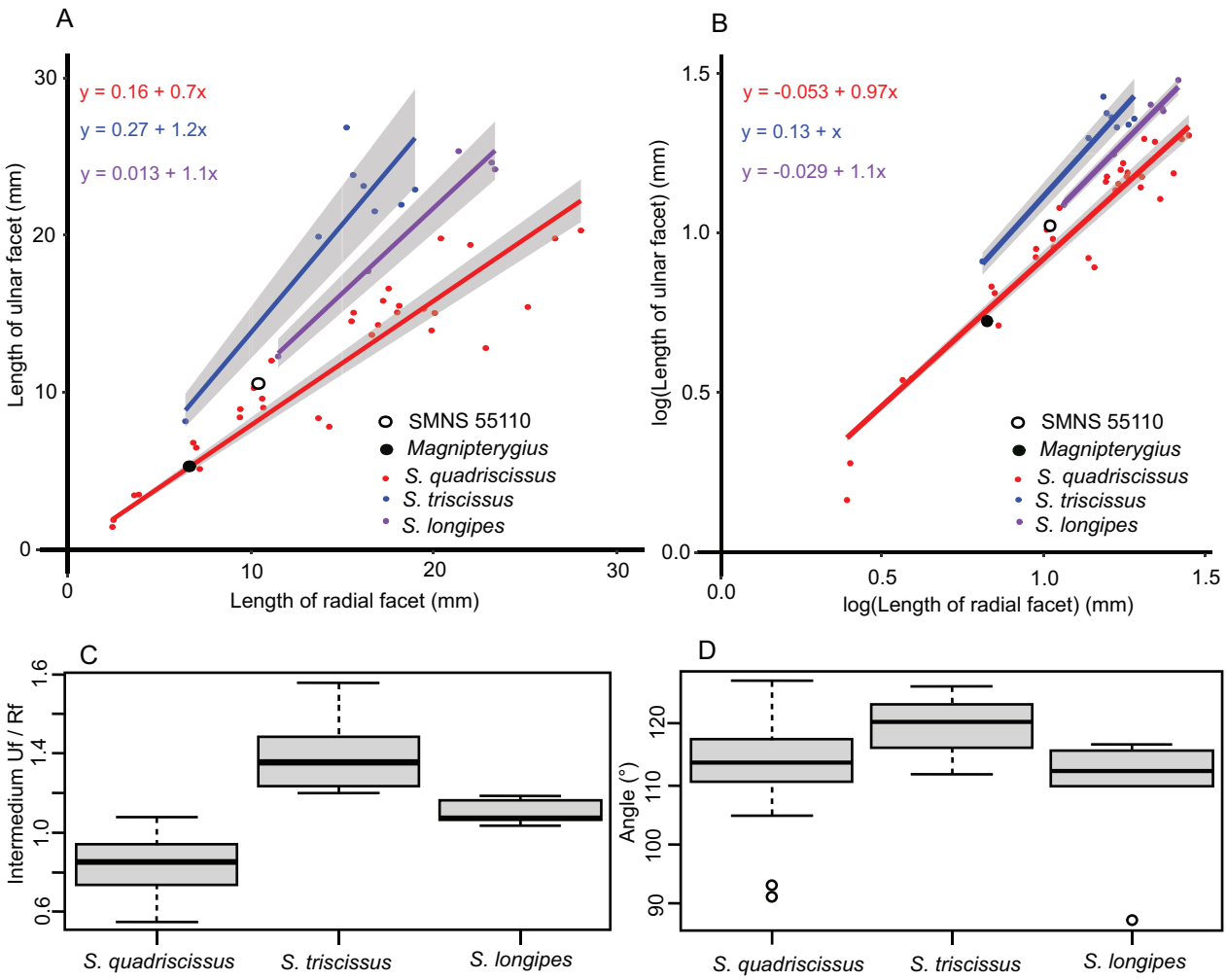

Figure 4. Intermedium measurements used to differentiate *Stenopterygius quadriscissus* (n = 31), *S. triscissus* (n = 9) and *S. longipes* (n = 6). **A, B.** Linear regression of the length of radial and ulnar facets of the intermedium (in mm); SMNS 55110 (Ravenscar ichthyosaur) and SMNS 96922 (holotype of *Magnipterygius huenei*) plotted for reference. **A.** Untransformed data; **B.** Log transformed data. Shaded areas represent the 95% confidence interval of the slope. **C.** Boxplot of the ratio of the ulnar facet (Uf)/radial facet (Rf) of the intermedium; **D.** Angle formed by the radial and ulnar facets of the intermedium; outliers denoted by circles.

Other species. *Stenopterygius triscissus*, *Stenopterygius longipes* (see Remarks), *Stenopterygius aaleniensis* (Maisch 2008; Maxwell 2012; Maxwell et al. 2012).

Diagnosis (modified from Maxwell (2012)). Upper temporal fenestrae large and wider anteriorly than posteriorly, unlike in *Hauffiopteryx* and *Eurhinosaurus*. Mandibular alveolar groove short in adults, not continuing posterior to mid-point of external nares. Suborbital groove on surangular long and deep, similar to *Ophthalmosaurus*, but unlike *Temnodontosaurus* and *Ichthyosaurus*. Angular exposure on posterior lower jaw extensive, but less so than in ophthalmosaurians. Crowns of teeth smooth, lacking macroscopic enamel ornamentation, unlike most ophthalmosaurians and *Ichthyosaurus*, but similar to *Eurhinosaurus* and *Hauffiopteryx*. Scapula with prominent acromial angle; posterior notch of coracoid reduced or absent, as in ophthalmosaurians, but unlike in *Ichthyosaurus*. Humerus with two distal facets, for articulation with the radius and ulna, shared with all non-ophthalmosaurian ichthyosaurs. Fore-limb with 4 digits, homologous to digits II–V, individual elements tightly packed proximally, notching in leading edge of some elements of the anterior digit shared with many non-ophthalmosaurian ichthyosaurs. Intermedium supporting primarily digit III (i.e. longipinnate, unlike *Ichthyosaurus* and *Ophthalmosaurus*). Pelvic girdle bipartite, ischium and pubis fused both medially and laterally to enclose the obturator foramen, shared only with some ophthalmosaurians. Hind-limb with three digits, notching in leading edge of some elements as in many non-ophthalmosaurian ichthyosaurs. Paired limbs disproportionate in length, fore-limb at least twice length of hind-limb, humerus approximately 30% longer than femur, shared with *Ichthyosaurus* and *Ophthalmosaurus*. Presacral vertebrae 44–46; preflexural vertebrae $80 < n < 90$, similar to *Hauffiopteryx* (45–46 presacral vertebrae and 81 preflexural vertebrae), but unlike in *Eurhinosaurus* (preflexural count > 95: McGowan and Motani (2003)) and *Ichthyosaurus* (preflexural count < 80: McGowan and Motani (2003); Massare and Lomax (2018)).

Remarks to *Stenopterygius longipes* (Wurstemberger, 1876).

The type material of *Stenopterygius longipes* consists of a large ichthyosaur skeleton, GPIT-PV-30019 (Stöhr and Werneburg (2022): pl. 4A), mounted on the wall near the ceiling at the GPIT. The specimen shows the classic 'head dive' taphonomic posture, with the anterior rostrum protruding out of the wall in three dimensions, the posterior portion of the skull including the orbits and upper temporal fenestrae compressed and distorted, the anterior vertebral column and rib cage acutely compressed and pushed into the back of the skull and the anterior forelimbs penetrating into the sediment (Martill 1993; Wahl 2009; Maxwell et al. 2022). Maisch (1998a) raised questions of specimen authenticity and used these grounds to invalidate *S. longipes* as a species. In particular, he considered the humeri as having been rotated proximodistally 180°, in addition to duplication of the right ulna and lack of zeugopodial elements on the left, suggesting the fore-limbs likely do not belong to the same individual as the rest of the skeleton. He concluded that since the fore-limbs likely do not belong with the rest of the skeleton, GPIT-PV-30019 is non-diagnostic and, therefore, declared *S. longipes* a nomen dubium (Maisch 1998a).

Maisch (1998a) noted that the hind-limbs of GPIT-PV-30019 showed a particular pathological pattern of fusion of proximal elements. However, he failed to note that the fore-limbs, most notably the right forelimb in which the radius, radiale and intermedium are partially co-ossified, show the same pattern of exostoses and pathological fusion of elements as the hind-limbs (Pardo-Pérez et al. (2019): cited as GPIT no. 83). Re-examination of the skeleton indicates that the humeri are exposed in anterior view, consistent with specimen taphonomy, with the distal end orientated correctly relative to the limb axis. The right humerus is badly fractured and differentially compacted; it is likely that one of the fragments is what Maisch interpreted as a duplicated ulna. In the left limb, the radius is preserved and in articulation with the distal limb elements, although partially overlapped by a fragment of a more posterior element, possibly the ulna. Therefore, it is clear that the fore-limbs and hind-limbs belong to the same individual and there is no reason to assume GPIT-PV-30019 is a composite – with the potential exception of the postflexural tail, a conclusion reached independently by other authors using different lines of evidence (Stöhr and Werneburg 2022).

GPIT-PV-30019 is a large individual of *Stenopterygius*. As preserved, the specimen is estimated to be at least 3.4 m in length (although the post-flexural tail may not belong to the same specimen: Stöhr and Werneburg (2022)), with a skull length of at least 550 mm (given the compaction of the orbital and cheek region, this is an underestimate); humeri approximately 123 mm in length and femora 96 mm in length. Although total and skull length cannot be accurately measured, the limb bones are far longer than those of the largest documented individual referable to *S. quadriscissus*; the femur, ischiopubis and hind-limb are too large and robust to be consistent with *S. triscissus*. The pectoral limbs are long and wing-like. For these reasons, we conclude that *Stenopterygius longipes* (Wurstemberger, 1876) is consistent with the current taxonomic concept of *Stenopterygius uniter* von Huene, 1931 sensu Maisch (2008) and, therefore, is the senior synonym.

Remarks to *Magnipterygius huenei* Maisch & Matzke, 2022.

Magnipterygius huenei, from the Posidonienschiefer Formation of Germany and represented only by its holotype SMNS 96922 (Fig. 5A), was described as a small stenopterygiid. It was diagnosed to the exclusion of other Toarcian *Stenopterygius* species by its small size, low number of presacral and preflexural vertebrae (36 presacral and 70 preflexural, according to Maisch and Matzke (2022)), a parietal foramen enclosed by frontals and pre- and postflexural caudal regions almost equal in length. Numerous comparisons of this specimen with *S. triscissus* were undertaken during the initial description (Maisch and Matzke 2022), but none with *S. quadriscissus*.

Maisch and Matzke (2022) considered SMNS 96922 to be at least subadult (= postnatal 2, osteologically immature adult: Miedema and Maxwell (2022)). However, the proximal articular surface of the humerus is flat, the humeral shaft has a roughened texture, the sutures between proximal forelimb elements remain open, the radius is unnotched and the notches on the proximal and distal carpals of digit II are weakly developed, all of which are consistent with postnatal stage 1 of *Stenopterygius* (Johnson 1977; Maxwell et al. 2014). In the skull, the parietal bears a dorsal triangular platform (Fig. 5C), present in postnatal stage 1 of *Stenopterygius*, but absent in later stages. The ossification centre of the parietal also remains visible, indicated by radiating bone fibres, and a weakly developed parietal shelf is present, both characters of which are consistent with postnatal stage 1, but not with more osteologically mature individuals. The jugal is semi-lunate to semi-angular, whereas it is very angular from postnatal stage 2 onwards. Some ontogenetic characters, diagnostic of postnatal stage 1, are also visible on the frontal, such as its more quadrangular outline, the interfrontal suture being less ossified and the absence of medial process anterior to the anterior border of the parietal foramen (Miedema and Maxwell 2022). In addition to these qualitative characters, skull length is estimated at 270 mm (Maisch and Matzke 2022), which is consistent with postnatal stage 1 of *Stenopterygius* (Miedema and Maxwell 2022). Therefore, the small body size in SMNS 96922 can be attributed to an earlier ontogenetic stage than previously inferred, rather than a species-level characteristic.

Magnipterygius huenei was diagnosed by a low vertebral count (36 presacral and 34 tailstock vertebrae according to Maisch and Matzke (2022)) relative to *S. triscissus*. The low presacral count can be attributed to taphonomic factors:

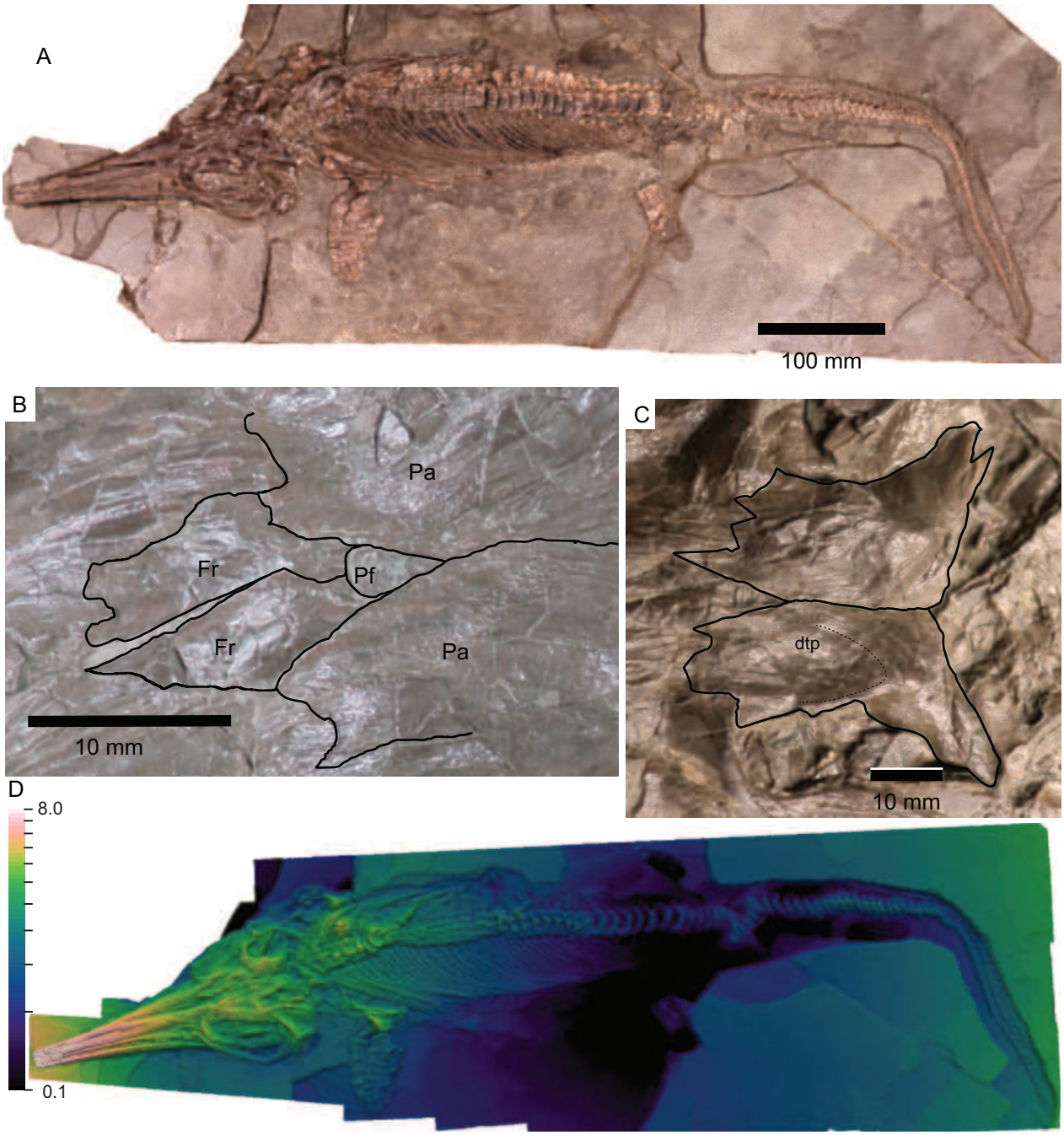

Figure 5. Holotype of *Magnipterygius huenei* (SMNS 96922). **A.** Overview photo; **B.** Interpretation of the parietal foramen; **C.** Parietal morphology; note the presence of the dorsal triangular platform and the absence of a well-defined parietal shelf and ridge. **D.** False-colour depth map, showing deeper embedding depth of the rostrum than any other part of the skeleton; specimen prepared from the underside. Depth map (in cm) indicated on a log scale. Abbreviations: dtp, dorsal triangular platform; Fr, frontal; Pa, parietal; Pf, parietal foramen. Photo (**A**) (copyright) M. Wahler/SMNS.

headfirst seafloor arrival in ichthyosaurs can displace the cervical centra inside the skull such that they are not externally visible (Maxwell et al. 2022; Johnson et al. 2025) and embedding depth of the anterior rostrum in SMNS 96922 clearly supports such a taphonomic interpretation (Fig. 5D). By counting the number of presacral ribs instead of centra, a count of 45 presacral vertebrae is obtained. Thirty-four tailstock vertebrae are present, which is not typically consistent with *S. triscissus* (Maisch and Matzke 2022), but well within the range of *S. quadriscissus* (Fig. 3D). The equal length of the postflexural region and tailstock was also cited as diagnostic for *Magnipterygius* to the exclusion of *S. triscissus*; a tailstock almost equal in length to the postflexural vertebral column is also characteristic of *S. quadriscissus*, which shows a longer postflexural region than *S. triscissus* (Fig. 3C). A more in-depth comparison with perinatal *S. quadriscissus* specimens gives similar results (postflexural length/total caudal length = 0.46 for SMNS 96922; vs. 0.47 for perinatal soft-tissue specimen of *S. quadriscissus* SMNS 12821).

Closer examination of the parietal foramen of SMNS 96922 (Fig. 5B) revealed that it is not totally enclosed by the frontals, with the parietals participating posteriorly (contra Maisch and Matzke (2022)), as in all *Stenopterygius* species (Lomax et al. 2020). A jugal–premaxillary contact, with the ventral border of the external nares only composed by the extensive subnarial process of the premaxilla was also cited as differentiating *Stenopterygius* and *Magnipterygius* (Maisch and Matzke 2022). However, as the lacrimal has clearly been anteriorly displaced from its articulation with the prefrontal (similar to SMNS 55110; see below); this anterior displacement has also affected the jugal, forcing it into contact with the subnarial process of the premaxilla and leading to the external nares being foreshortened. This type of displacement is typical of head-first arrival specimens (Wahl 2009; reviewed by Johnson et al. (2025)). The absence of a sagittal crest and the flat appearance of the parietal are due to ontogeny (see above). Finally, the scapula to does not appear any more slender than in other scapulae of juvenile *Stenopterygius* (pers. observ. FM).

Lastly, Maisch and Matzke (2022) cited the posterior insertion of the soft tissue dorsal fin, beginning at the 39th presacral centrum (= 30th of Maisch and Matzke (2022)), with the apex situated opposite or posterior to the presacral-caudal transition. In comparison, in other *Stenopterygius* specimens, the dorsal fin inserts more anteriorly and the apex is well anterior to the presacral-caudal transition. While the position of the apex appears to be somewhat ontogenetically dependent (e.g. the apex is opposite or near-opposite the presacral-caudal transition in perinatal specimens, for example, SMNS 12821), the anterior insertion is around centrum ~ 32; i.e. still well anterior to that of *Magnipterygius*. In the absence of osteological differences, soft-tissue slippage during decay appears to be the most plausible explanation.

In addition to the similarities with *Stenopterygius quadriscissus* in caudal proportions, the length of the ulnar facet is inferior to the length of the radial facet of the intermedium in SMNS 96922 (Uf/Rf = 0.79); this value is only consistent with *S. quadriscissus* amongst Toarcian species of *Stenopterygius*.

Therefore, based on both ontogenetic and qualitative criteria, *Magnipterygius huenei* cannot be differentiated from *Stenopterygius quadriscissus* and we consider *M. huenei* to be a subjective junior synonym of the latter taxon.

Stenopterygius quadriscissus (Quenstedt, 1856)

Partial synonymy.

Stenopterygius eos von Huene, 1931: Fraas 1891 pl. 4, fig. 1 (lectotype sensu Maisch (2008)).

Stenopterygius incessus von Huene, 1931: pl. 1, fig. 1.

Stenopterygius promegacephalus von Huene, 1949: Maisch (2008) pl. 8, fig. 1.

Stenopterygius macrophasma McGowan, 1979: pl. 3, fig. 2.

Magnipterygius huenei Maisch & Matzke, 2022: p. 170, figs 2–12.

Lectotype. GPIT-PV-30028; for a list of paralectotypes, see Hungerbühler (1994).

Diagnosis. Modified from Maxwell (2012); characters indicated by an asterisk are new. Moderately large form, maximum length approximately 3.5 m, antorbital segment moderately long, approximately two-thirds the length of the lower jaw; tooth reduction in individuals greater than 2 m total length; forelimb shorter than in *Stenopterygius longipes*, longer than in *S. triscissus*; ulnar facet of intermedium usually shorter than radial facet ***** (ratio usually < 1 and never > 1.07; radial facet longer in *S. triscissus* (1.20–1.75) and *S. longipes* (1.03–1.18)); premaxilla and lower jaw shorter relative to length of humerus, femur, scapula and ischiopubis than in *S. longipes* or *S. triscissus*. In osteologically mature individuals, distal tarsal II strongly notched with smaller surface area than the astragalus or calcaneum, unlike in *S. longipes*; body deeper than *S. longipes* and *S. triscissus*; tailstock vertebral count 34–40 in adults and large juveniles ***** (mean = 35.6; higher in *S. triscissus*: 34–44, mean = 39.8); postflexural length 0.35–0.44 total caudal length in adults ***** (reduced in *S. triscissus*: 0.31–0.36).

Remarks. Juvenile *S. quadriscissus* (specimens with lower jaw lengths between 200 and 400 mm) can have a relative postflexural length either longer or shorter than adult individuals (ratio to total caudal length = 0.34–0.47). If the length of the ulnar facet of the intermedium is longer than the radial facet (Uf/Rf = 1.0–1.07), comparisons with *S. longipes* are necessary to correctly refer a specimen to species.

Description of SMNS 55110, the Ravenscar *Stenopterygius*.

SMNS 55110 is a nearly complete articulated skeleton exposed on its right lateral side for most of the body length (Fig. 6A). The skull is exposed ventro-laterally, revealing the mandible, but not the majority of skull roof. The fore-limbs and the pectoral girdle have become detached from the axial skeleton, as have the majority of the ribs. Nevertheless, the fore-limbs and the pectoral girdle remain completely articulated as an anatomical unit. The hind-limbs and the pelvic girdle are missing. Some parts of the posterodorsal skull are also disarticulated, including both scleral rings, supratemporals and postorbitals and the left postfrontal, quadrate and squamosal. The total length of the specimen is 145.8 cm (Table 1). It is worth noting that the excellent preservation of the specimen is only highlighted due to the excellent preparation of the skeleton, something that most historical specimens lack. More recently collected material from the Whitby area residing in private collections is similarly well-prepared and displays similar levels of preservation (DRL pers. obs.).

Skull

The skull is moderately flattened dorso-ventrally and the jaws are agape, exposing the ventral surface of the premaxillae. The snout ratio (sensu McGowan (1976)) is 0.74 and the orbital ratio (sensu McGowan (1976)) is 0.20.

The premaxilla (Fig. 7A, B) forms the majority of the rostrum. The right premaxilla is exposed in ventrolateral view and the left in ventral view. In ventral view, the premaxillae form an acutely pointed rostrum, separated on the mid-line by a butt joint formed by the articulation of the contralateral elements. Anteriorly, no overbite is present (unlike in *Hauffiopteryx* (slight) or *Eurhinosaurus*, *Excalibosaurus* (substantial): McGowan 1989; McGowan 1994; Maxwell and Cortés 2020). Posteriorly, the right premaxilla has been broken and dorsally displaced and is exposed in lateral view. It articulates with the maxilla posteroventrally and forms the anteroventral edge of the external nares. The left alveolar groove of the premaxilla (Fig. 7A, B) is visible in ventral view; posteriorly it is covered by matrix. Pseudoalveoli (sensu Bennion et al. (2024)) are visible in ventral view; the size of tooth impressions increases posteriorly.

The maxilla (Fig. 7A, B) has an elongate triangular outline and is smooth in lateral view; its deepest point occurs ventral to the subnarial process of the premaxilla at the anterior edge of the external nares. This positioning is likely due to taphonomic displacement, as the maxilla and posterior premaxilla have been ventro-anteriorly displaced. The ventrolateral edge of the maxilla is gently concave in lateral view. The posteriormost part of the maxilla is broken and is in contact in lateral view with the lacrimal dorsally and with the anterior jugal posteriorly and ventrally. Despite the alveolar groove remaining covered in sediment, some teeth are preserved lying ventral to the maxilla.

The nasals (Fig. 7A, B) are not completely exposed; only a small part of the lateral face of the right nasal is visible in lateral view dorsal to the anterior external nares and extending posteriorly to the mid-point of the prefrontal.

The lacrimal has been taphonomically displaced into the external narial opening. It is triangular in lateral view and contacts the posterodorsal maxilla for about 1/4 of the total length of the latter (Fig. 7A, B). The anterior lacrimal contributes to the ventral margin of the external nares with its concave dorsal edge. The anteriormost lacrimal may contact the end of the subnarial process of the premaxilla, but this is not certain due to displacement of both bones. Dorsally, the lacrimal would have articulated with the prefrontal; the sutural contact is visible although displacement has shifted the lacrimal anteriorly. The ventral border of the posterior lacrimal extends ventral to the anterior third of the orbit in lateral view.

Below the posterior lacrimal is a fragment of the anterior jugal (Fig. 7A, B), which has been displaced and now situated ventral to the surangular.

The right prefrontal (Fig. 7A, B), exposed in lateroventral view, shows some damage to its lateral edge and, together with the lacrimal, forms the anterior margin of the orbit. The prefrontal is excluded by the lacrimal and nasal from the posterior edge of the external nares (unlike in *Hauffiopteryx*: Maxwell and Cortés (2020)). The prefrontal contacts the postfrontal posteriorly and the nasal medially and anteriorly; the total medial contact with the nasal is not visible since the skull remains embedded in sediment. The prefrontal-nasal suture trends from anterolateral to posteromedial, so the prefrontal is wider in its posterior part. The anterior prefrontal appears thin and becomes thicker posteriorly. The ventral border of the prefrontal is concave in lateral view, as it forms the dorsal margin of the orbit; the laterodorsal edge of the prefrontal appears convex. The posteromedial prefrontal is not exposed.

Dorsal to the orbit, part of the right postfrontal is exposed in lateroventral view, still in articulation with the rest of the skull (Fig. 7A, B), but its lateral edge has been damaged. The postfrontal articulates with the prefrontal anteriorly; posteriorly, it would articulate with the anterior ramus of the supratemporal, although the latter is not in articulation. The postfrontal is smooth and the suture with the prefrontal is easily visible. The ventral surface of the postfrontal is concave; the dorsolateral surface is convex. The postfrontal is ventrodorsally thickened, marking the medial edge of the orbital cavity. This ventral ridge is slender anteriorly and becomes wider posteriorly. The ventral surface of the lateral flange is widest anteriorly and becomes thinner posteriorly. A deep groove separates the ventral ridge and lateral flange. The left postfrontal is preserved in ventral view, overlying the right forelimb (Fig. 6B). The bone is anteriorly broad, narrowing posteriorly. The lateral edge has been damaged; the medial edge forming the lateral wall of the upper temporal fenestra is concave. Anteriorly, a prominent, roughened prefrontal facet forms a depression in the anterior ventral ridge. The ventral ridge narrows, becoming constrained to the medial edge of the bone posteriorly. The narrow posterior postfrontal preserves the anteriormost part of the interdigitating sutural contact with the supratemporal.

The right supratemporal is displaced from the skull, but is easily recognisable, preserved in dorsal view (Fig. 6D). It exposes a damaged anterior ramus, a triangular medial ramus and part of the ventral ramus. The anterior and medial rami form the posterior edges of the upper temporal fenestra and both have relatively straight edges on the side of the fenestra, unlike in *Hauffiopteryx* and *Eurhinosaurus* in which the anterior ramus has a medial edge that gently curves medially, due to the reduced size of the fenestra (see, for example, Marek et al. (2015)). The left supratemporal is preserved in the same displaced cluster of bones. It exposes a damaged ventral ramus, the triangular medial ramus and a part of the anterior ramus covered by the left postorbital.

The postorbitals (in lateral view) are not articulated with the skull (Fig. 6D), having been displaced posteriorly, similar to the supratemporals. The posterodorsal postorbital contribution to the orbital margin is formed by a wide, transverse flange dorsally forming the postfrontal facet and the posterior lamella including the squamosal facet, which gives a nearly square outline to the dorsal surface of the postorbital. The anterior postorbital is concave while the posterior margin appears convex. The circumorbital area is well-defined dorsally by an anterodorsal-posteroventrally trending ridge, which terminates at the quadratojugal facet.

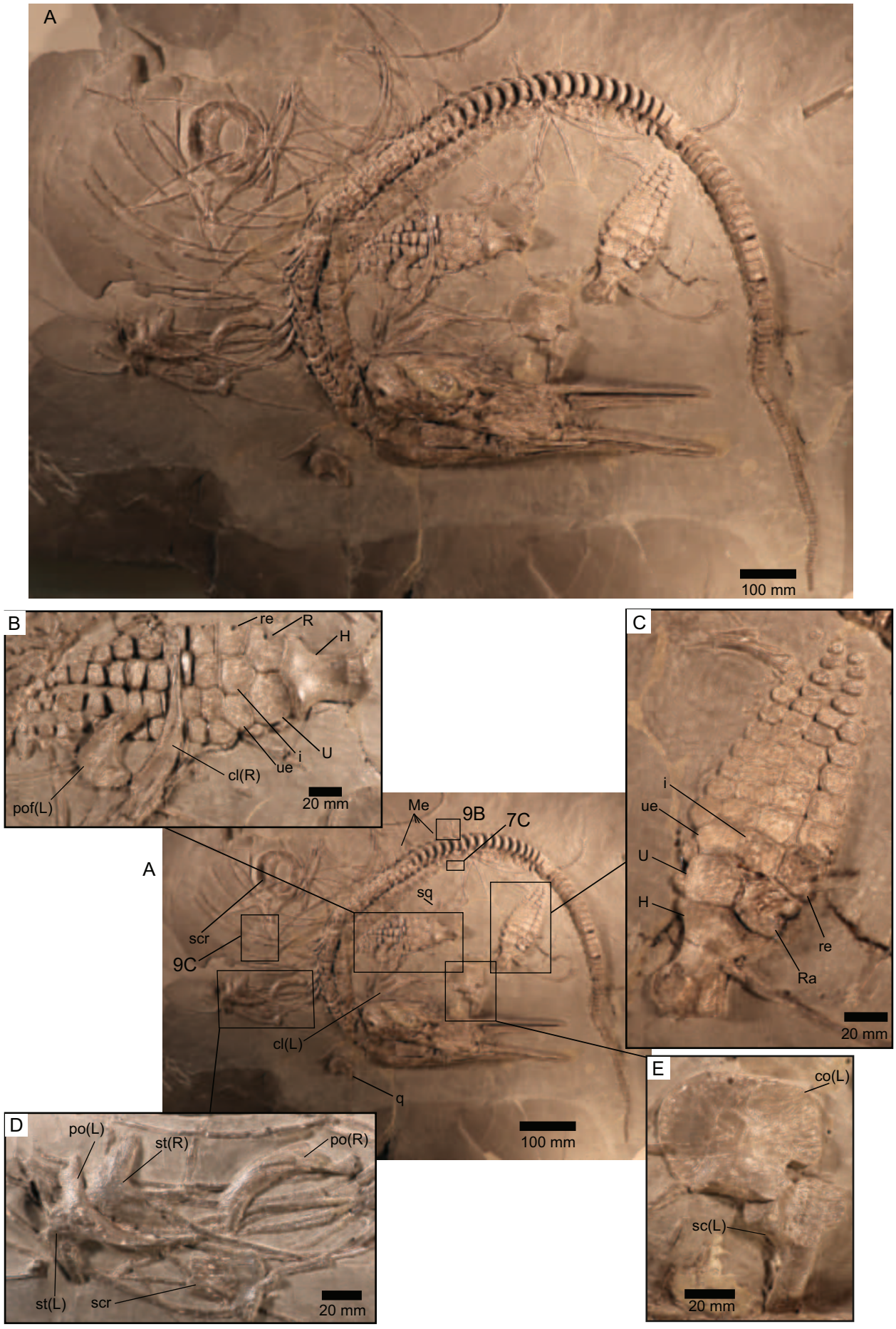
A
100 mm
B
re
R
H
i
U
ue
cl(R)
pof(L)
20 mm
Me
9B
7C
sq
scr
9C
cl(L)
q
100 mm
C
i
ue
U
H
re
Ra
20 mm
D
po(L)
st(R)
po(R)
st(L)
scr
20 mm
E
co(L)
sc(L)
20 mm

The left squamosal is exposed in medial view, situated above the left fore-limb. As it is not in articulation and covered by other bones, the articular facet for the quadratojugal is clearly visible with roughened surfaces. This surface extends over most of the anteroventral squamosal, being limited posterodorsally by a ridge. Posterodorsal to this ridge is the quadrate facet, which appears quite smooth compared to the quadratojugal facet. The posterior edge of the squamosal is thickened and ventrally concave, forming the lateral edge of the quadrate foramen.

The left quadrate lies posterior to the skull (Fig. 6A), below it on the slab. The quadrate is more slender dorsally than ventrally and here exposes its smooth lateral face. It has a convex anterior margin and a concave posterolateral margin. The ventral surface of the quadrate bears the articular condyle and its edge can be observed in ventrolateral view. The anterior and posterior bosses are not well developed and the articular condyle appears as a single structure, as in prenatal and early postnatal stages (Miedema and Maxwell 2019).

The basioccipital is exposed in ventral view (Fig. 7A, B), in articulation with the atlas-axis complex. The edge of the condyle is visible posteriorly and, anterior to the condyle, the smooth extracondylar area extends anteroventrally and laterally. Anterior to the extracondylar area, a rugose texture is present and corresponds to the stapedial facet, the majority of which is not exposed.

Below the stapedial facet of the basioccipital is the right stapes (Fig. 7A, B), exposed in posterolateral view. The medial head of the stapes remains articulated with the basioccipital, while the quadrate facet is directed more anteriorly than laterally, indicating that the stapes was slightly displaced during burial. In lateral view, the edge of the hyoid process situated ventrally on the stapedial head is visible.

The quadrate ramus of the right pterygoid (Fig. 7A, B) is present, but is poorly preserved in ventral view. It is exposed medial to the prearticular and lateral to the basisphenoid. The lateral flange of the quadrate ramus is partially covered by the prearticular; the other flanges are not visible. A portion of the palatal ramus of the left pterygoid is preserved in the palatal region, exposing the postpalatine process. Anterior to the pterygoid, an unidentified element is exposed.

The parabasisphenoid (Fig. 7A, B) is preserved anterior to the basioccipital in dorsal view. The right impression of the trabecular cartilage is visible and extends from the body of the basisphenoid to the cultriform process. The right basipterygoid process is well visible, but the left is mostly hidden. The dorsum sellae extend dorsally posterior to the parasphenoid, but other details of this area are not visible due to poor preservation. The cultriform process, likely visible due to compaction, extends from the anterior ventral margin of the parabasisphenoid, but is broken near the posterior edge of the right splenial.

The right surangular (Fig. 7A, B), visible in lateral view, is a long bone, extending anteriorly from the most posterior part of the lower jaw. It is broken ventral to the anterior orbit and disappears in lateral view. The surangular is weakly curved below mid-orbit and is broken in several parts. This dorsal curve is created by the paracoronoid process, situated just anterior to the break on the dorsal margin and by the preglenoid process, situated just posterior to the break and visible as a small bump on the dorsal surface. These two processes are in close proximity, but can be distinguished because of the break present in the area. Below these two processes, traces of the surangular foramen are visible. The majority of the ventrolateral surangular is covered by the angular. The left surangular is also exposed in lateral view; it extends approximately as far anteriorly as the deepest point of the maxilla, posterior to the mandibular symphysis.

The right angular (Fig. 7A, B) covers the ventral surangular in lateral view. The angular appears posterior to the mandibular symphysis, slightly anterior to the surangular and becomes deeper posteriorly until it covers much of the ventral surangular. However, the exposure of the angular is not as extensive as in *Ophthalmosaurus* (Moon and Kirton 2016). The left angular is also visible in ventral view, lateral to the splenial. The posterior third is missing.

The dentary is narrow and slender in ventrolateral view (Fig. 7A, B), becoming deeper posteriorly in lateral view. The dentary fossa extends over the anterior two-thirds of the lateral surface. The ventral edge of the posterior dentary contacts the dorsal angular over a small contact and, posterior to this, the surangular. The lower jaw is similar in size and length to the upper jaw; no overbite is present. The dentaries make up 58% of the length of the mandibular symphysis (10.1 cm /17.4 cm), with the remainder being formed by the splenials.

The splenials are exposed in ventral view (Fig. 7A, B), situated medial to the dentary and forming the posterior part of the mandibular symphysis. The left splenial, in ventromedial view, appears at ~ 33% of dentary length and extends posteriorly along the medial surface of the lower jaw until around the mid-point of the orbit. The right splenial appears in the same position, but is excluded in lateral view by the angular ventral to the lacrimal. In ventromedial view, the left splenial bears a rugose area on its medial surface, marking its participation in the mandibular symphysis (Andrews 1910; Moon and Kirton 2016).

The right prearticular is situated in the posteriormost part of the lower jaw, medial to the angular in ventral view. It appears as a thin bone; anteriorly, it is covered by the splenial.

Figure 6. SMNS 55110, *Stenopterygius quadriscissus*. **A.** Overview; **B.** Right fore-limb, ventral view; **C.** Left fore-limb, dorsal view; **D.** Disarticulated bones from the cheek region; **E.** Left pectoral girdle, external view. Abbreviations: cl, clavicle; co, coracoid; H, humerus; i, intermedium; Me, additional *Meleagrinella* valves; po, postorbital; pof, postfrontal; q, quadrate; R, radius; re, radiale; sc, scapula; scr, scleral plates/scleral ring; sq, squamosal; st, supratemporal; U, ulna; ue, ulnare.

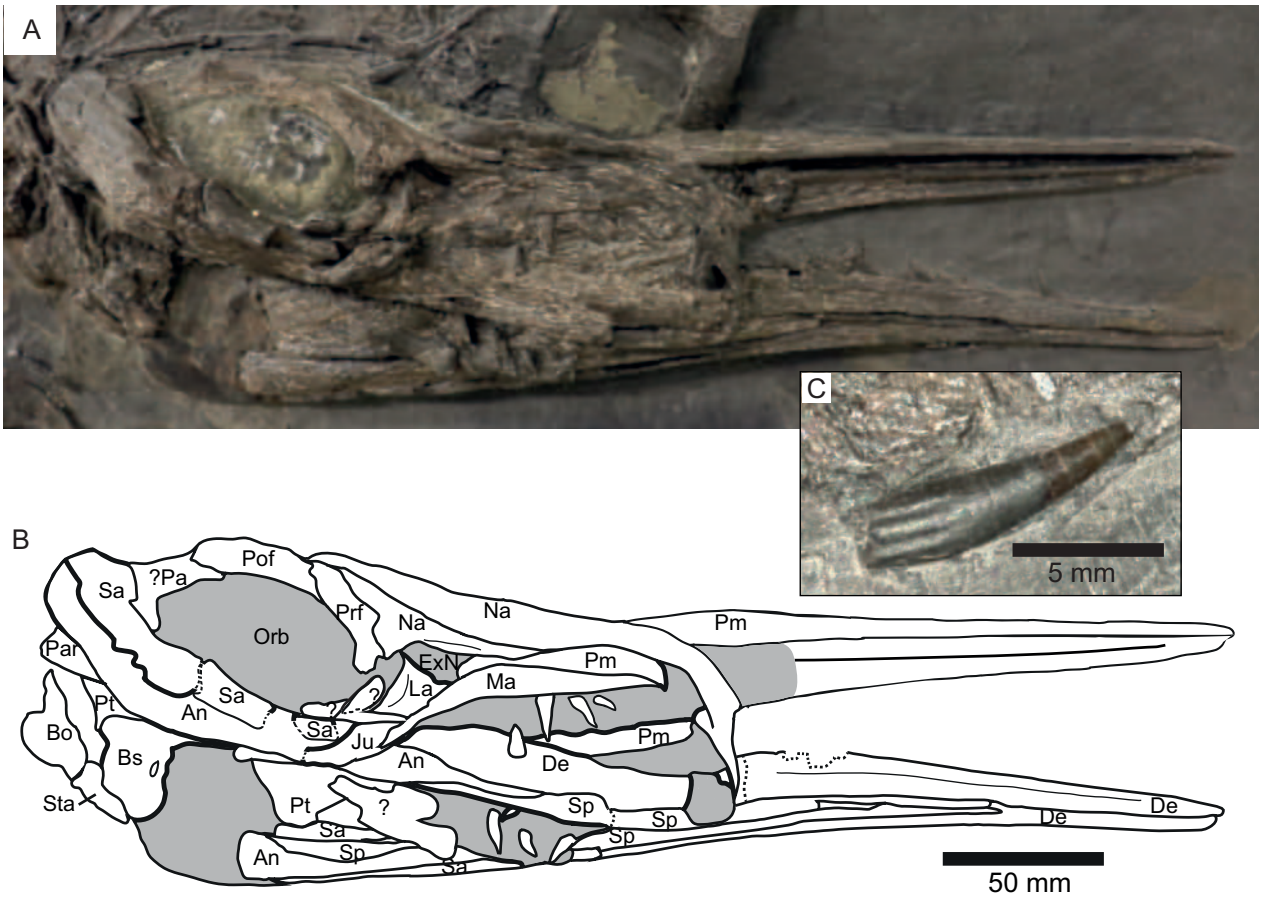

Figure 7. Skull of *Stenopterygius quadriscissus* (SMNS 55110), ventro-laterally exposed. **A.** Photograph; **B.** interpretive drawing; **C.** well-preserved tooth showing dentine infolding at base; for location on slab, see Fig. 6A. Abbreviations: An, angular; Bo, basioccipital; Bs, basisphenoid; De, dentary; ExN, external nares; Ju, jugal; La, lacrimal; Ma, maxilla; Na, nasal; Orb, orbit; Pa, parietal; Pm, premaxilla; Pof, postfrontal; Par, prearticular; Prf, prefrontal; Pt, pterygoid; Sa, surangular; Sp, splenial; Sta, stapes.

At least 12 teeth (Fig. 7A, B) are preserved in the vicinity of the jaws, mostly in labial view. These are about 10 mm in total height. Additional teeth are preserved inside the curve formed by the vertebral column; these are, for the most part, better-preserved than those in the jaws. The crowns (about 4 mm high) are smooth, lacking apicobasal enamel ridges, with a diameter at the base of the crown of ca. 1.6 mm (vs. 3 mm root diameter). The teeth are round in cross-section and bear deep apicobasal grooves on the roots indicating the presence of plicidentine. These do not reach the base of the crown (Fig. 7C).

The scleral ring, exposed in medial view, is composed of 14 plates and has been displaced towards the top of the slab. It presents an ovoid aperture 30 mm deep and 23.7 mm long and a total scleral ring length of 68.4 mm. Based on these measurements, the orbital ratio = 0.20. Isolated scleral plates are preserved near the supratemporals.

Postcranial axial skeleton

The vertebral column is complete and articulated; only the ribs are disarticulated (Fig. 6A). There are a total of 46 presacral vertebrae, all well exposed in lateral to ventral view. Centrum 47 appears to be the first caudal, based on the presence of a synapophysis (McGowan and Motani 2003). There are a total of 34 tailstock vertebrae and, therefore, 80 preflexural vertebrae are present. Seven apical centra are present and at least 54 postflexural vertebrae are preserved, leading to a total count of 134 vertebrae. The majority of centra are well preserved and well-ossified, including the di- and parapophyses. Posterior to the presacral-caudal transition, the first ten caudal vertebrae are of constant size; more posteriorly, the caudal centra become smaller both in length and height (Fig. 8). All the neural arches of the dorsal vertebrae are preserved and articulated; these become anteroposteriorly longer moving posteriorly along the vertebral column, until they disappear due to the position of the specimen. The caudal neural arches, when visible, follow the same size reduction. No ossified haemal arches are preserved; haemapophyses are likewise absent.

The fused atlas and axis are seen in right lateral view, separated by a prominent ridge on the lateral surface. The parapophyses are large. The neural arches of the atlas and the axis are about half of the height of their centra and the neural spines are directed dorsally. The axis neural spine is about 67% as tall as the centrum is long.

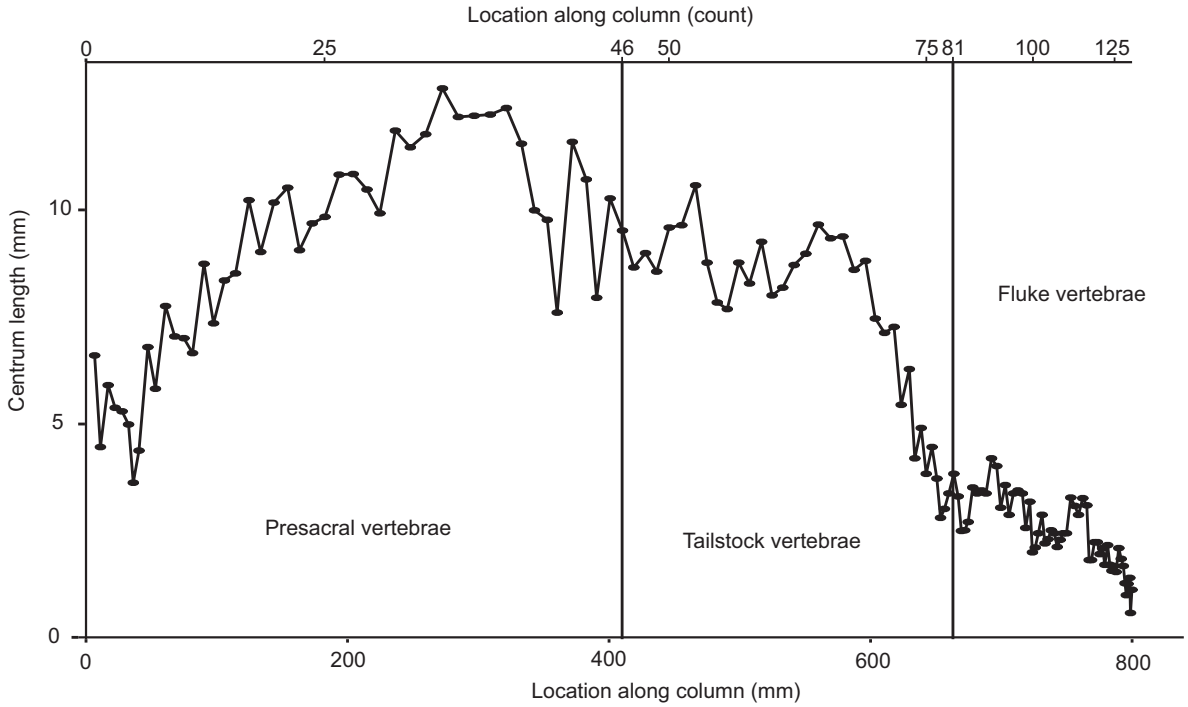

Figure 8. Vertebral column regionalisation in *Stenopterygius quadriscissus* (SMNS 55110).

The left ribs are preserved in articulation while the right ribs are disarticulated. Only presacral ribs are preserved; caudal ribs are missing. One rib from the anterior dorsal region (sensu Moon and Kirton (2016)) is well exposed in anterior view next to the right fore-limb; the larger capitulum and the smaller tuberculum are deflected dorsally, give the ribs a Y-shaped proximal end (see also Fig. 9B). This rib first extends dorsolaterally and then curves ventrally; this is less visible on the other anterior dorsal ribs as they are preserved in lateral view. Another well exposed anterior dorsal rib is present above the vertebral column, also in anterior view, where this curvature is clearly evident. Despite being exposed in anterior view, the longitudinal groove is not visible. The other ribs preserved are posterior dorsal ribs and are shorter than the anterior dorsal ribs. Their proximal ends cannot be observed as the majority are from the left side and so are articulated and under the centra. A series of at least four mid-dorsal ribs show evidence for callus formation at mid-shaft (Fig. 9C), indicating traumatic injury sustained during the life of the ichthyosaur. Traumatic injury to the ribs occurs commonly in juvenile *Stenopterygius* specimens (Pardo-Pérez et al. 2019).

Disarticulated gastralia are preserved, the most complete of which is situated to the right of the left fore-limb.

Pectoral girdle and fore-limbs

The majority of the pectoral girdle is preserved, lacking only the right coracoid, scapula and the interclavicle. The fore-limbs are both well preserved, the left being exposed in dorsal view and the right in ventral view.

The left coracoid, visible in ventral view, remains articulated with the scapula (Fig. 6E). The coracoid is longer than wide, giving it an ovoid aspect. The lateral glenoid facet and medial intercoracoid facet are slightly raised, giving to the coracoid a saddle shape. A well-developed anterior notch is present; a posterior notch is absent. The scapular facet is 11 mm long and is orientated anterolaterally, distinctly offset from and smaller than the glenoid. Posterior to the scapular facet, the glenoid facet of the coracoid is 31.5 mm in length, about 3 times longer than the scapular facet of the coracoid. The medial intercoracoid facet is 37.8 mm in length.

The scapula, visible in external view, remains in articulation with the coracoid (Fig. 6E). The proximal scapula is broad, with a prominent acromial process; the distal scapula is slender. The proximal scapula is concave, forming an S-shape created by the glenoid facet posterolaterally, the coracoid facet anteromedially and the acromion process anterolaterally. Posterolaterally, the glenoid facet of the scapula is concave, about 9 mm in length, while the coracoid facet is ca. 12 mm long. The scapula of *Stenopterygius* can have a third articular facet (Johnson 1979); however, this is not present in SMNS 55110, potentially for ontogenetic reasons. A small concave depression on the anteromedial margin of the scapula, posterior to the acromion process may represent this facet. The acromion process has a straight anterior margin that articulates with the posterior clavicle. Distal to the acromion process, the scapula becomes thinner, with a markedly concave posterior margin and a small concavity posterior to the acromion process. In cross-section, the distal shaft of the scapula is strap-like. In dorsal view, the lateral surface of the shaft is smooth, while the surface of the proximal expansion is roughened for muscle insertion.

Both clavicles are preserved, the right one overlying the right fore-limb and exposed in posterior view

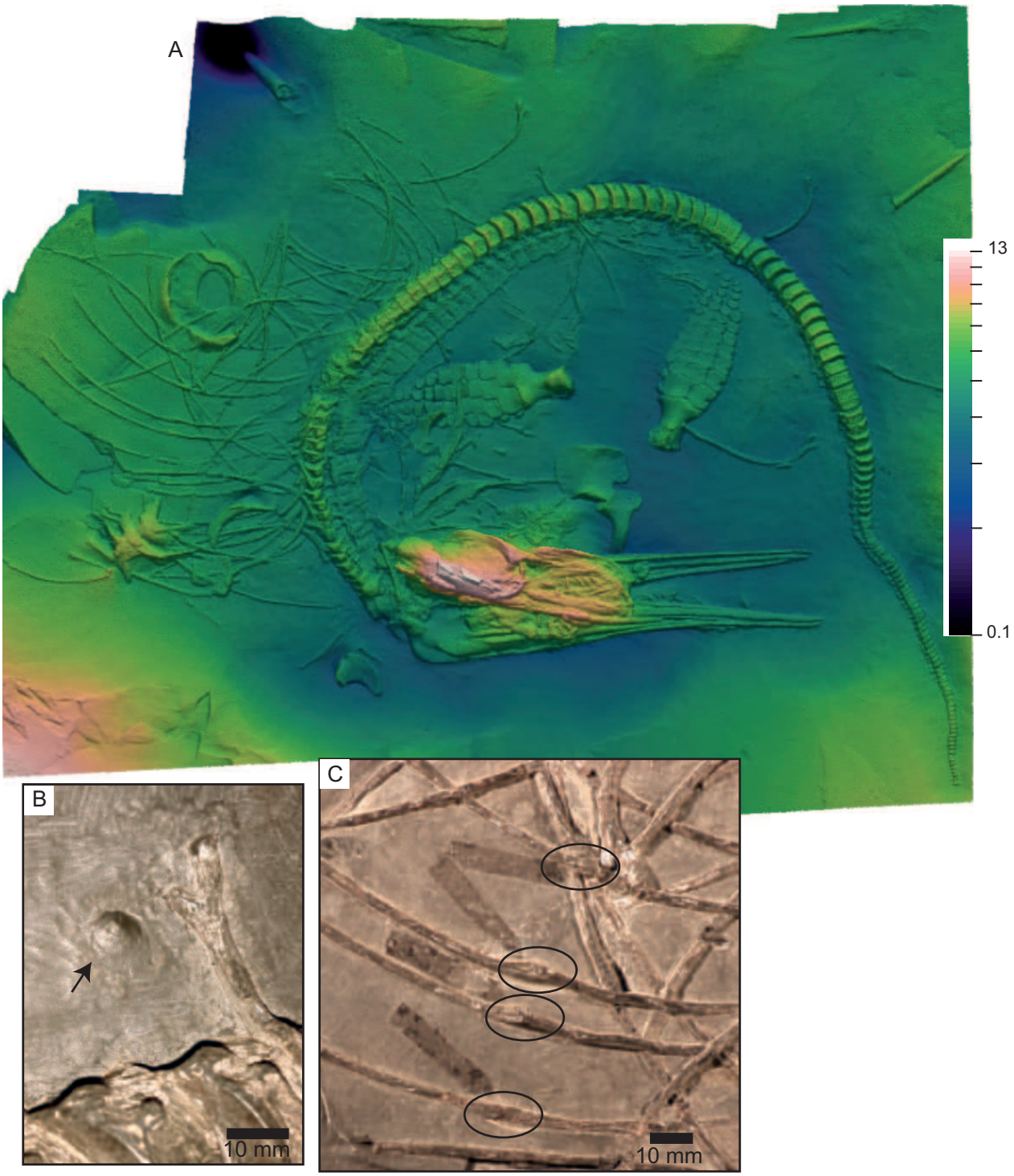

Figure 9. *Stenopterygius quadriscissus* (SMNS 55110), taphonomy and pathology. **A.** False-colour depth map, showing relative embedding depths of the ichthyosaur skeleton; specimen prepared from the upper surface; **B.** Example of *Meleagrinella* (arrow) with the umbo directed towards the top of the slab and a bicapitate dorsal rib near the posterodorsal vertebral column; for location on slab, see Fig. 6A; **C.** Dorsal ribs with callus development; for location on slab, see Fig. 6A. Depth map (in cm) indicated on a log scale.

(Fig. 6B), while the left clavicle is situated above the skull, also in posterior view (Fig. 6A). The clavicles are curved, with a proximally expanded lamina and become slender distally. The medial groove for articulation with the transverse bar of the interclavicle is clearly visible, best preserved on the left. The interclavicle facet has a roughened texture. Dorsally, the medial clavicles present a thick ridge where they wrap around the transverse bar of the interclavicle. Laterally, the clavicles show a concavity for articulation with the acromion process of the scapula; more dorsally, this forms a groove that continues until the most dorsal part of the clavicle, which is deeply roughened for articulation with the dorsal margin of the scapula.

Both fore-limbs (left fore-limb above the coracoid and right underlying the right clavicle; Fig. 6B, C) are complete, exposing the humerus, ulna, radius, carpals, metacarpals and phalanges. The left humerus is exposed in dorsal view (Fig. 6C). The humerus is short and robust and is wider distally than proximally with a well-defined shaft. The head of the humerus is convex and roughened, indicating articular cartilage. The dorsal trochanter is narrow and distinct, but poorly developed. The distal radial and ulnar facets are concave. The right humerus is exposed in ventral view (Fig. 6B) and is similar in shape of the left humerus. The deltopectoral crest creates a ridge that is not offset from the humeral shaft and shows a roughened area for the insertion of the scapulohumeralis muscle (Johnson 1979).

The radius is pentagonal in shape and is anteroposteriorly wider than proximodistally long. The anterior radius bears a deep notch. The radius articulates with the ulna posteriorly, the intermedium posterodistally and the radiale anterodistally. The ulna is also pentagonal and wider than long. It articulates with the intermedium anterodistally and the ulnare distally. The posterior margin is slightly convex and articulates with a small proximal ossicle situated immediately distal to the humerus and distally with the similar-sized pisiform, situated posterior to the articulation with the ulnare. The sutures between the elements are closed.

In the proximal carpal row, the radiale is roughly quadrangular in shape, wider than long and bears a notch on its anterior margin. Proximally, the radiale articulates with the radius, posteriorly with the intermedium, posterodistally is a small articulation with distal carpal 3 and distally with distal carpal 2. The intermedium is roughly pentagonal in shape. Its facets for articulation with the ulna and the radius are equal in length (10.4 mm for the articulation with the radius and 10.5 mm for the articulation with the ulna; Uf/Rf = 1.01). Anteriorly, the intermedium articulates with the radiale, posteriorly with the ulnare, distally with distal carpal 3 and, posterodistally, it bears a small facet for articulation with distal carpal 4. The ulnare is pentagonal in shape, wider than long and articulates anteriorly with the intermedium, proximally with the ulna, proximoposteriorly with the pisiform, posterodistally with metacarpal V and distally with distal carpal 4.

Four elements are present in the distal carpal row. Distal carpal 2 is similar to the radiale, with a notch present on its anterior margin and a roughly quadrangular shape; distal carpals 3 and 4 are also roughly quadrangular in shape. Distal carpals 2–4 are wider than long, whereas metacarpal V is the smallest element in the row and as long as wide. Distal carpal II articulates distally with only metacarpal II in the left limb, but bears a small posterodistal facet for metacarpal III on the right side; distal carpal III articulates with metacarpal III and also has a small posterodistal facet for metacarpal IV, distal carpal IV articulates with metacarpal IV and the first phalanx of digit V and metacarpal V articulates the first phalanx of digit V. The sutures between these elements are also closed.

Metacarpals II-IV are similar in shape and size to the distal carpal row. Metacarpal II is anteriorly notched. Each metacarpal supports a digit. Digit II is the functionally shortest digit and has four phalanges on the left and five on the right. The proximal phalanx is unnotched on the left, but notched on the right. Digit III preserves eight phalanges on the left, but potentially more on the right; digit IV preserves nine phalanges on the left and potentially more on the right; digit V preserves seven phalanges on the left, but at least 11 on the right. As the vertebral column overlaps the more complete right limb, it was not possible to assess which digit is the longest. The more distal phalanges are rounded and widely spaced. Starting from the fifth phalanx of digit V, at least three small posterior accessory ossicles are preserved on the left; none is visible on the right.

Table 1. Skeletal measurements of SMNS 55110 (in mm).

	Measurement (mm)
Total length	1458
Lower jaw (length)	337.1
Premaxilla (length)	208.4
Snout (length)	252.6
Scleral ring (length)	67.9
Scleral ring (depth)	74
Aperture (length)	30
Total caudal length	827.5
Tailstock length	583.9
Postflexural length	243.6
Fore-limb length	L : 157.7 /R : 156.4
Humerus length	L : 47.7 / R : 49.6
Humerus proximal width	L : 20.6 / R : 26.8
Humerus distal width	L : 38.9 / R : 38.1
Radius (length)	L : 21 / R : 20
Radius (width)	L : 24 / R : 21
Ulna (length)	L : 21 / R : 19
Ulna (width)	L : 23 / R : 22
Radiale (length)	L : 18.5 / R : 15
Radiale (width)	L : 17.8 / R : 17
Ulnare (length)	L : 16.1 / R : 16
Ulnare (width)	L : 16.7 / R : 15.5
Radial facet of intermedium	L : 10.4 / R : 10.3
Ulnar facet of intermedium	L : 10.5 / R : 10.2

Ontogeny

The length of the jaw (337 mm) indicates that the specimen is smaller than the smallest sexually mature individual of *S. quadriscissus* (McGowan 1979) and consistent with postnatal stage 2 (Miedema and Maxwell 2022). Osteologically, the humerus is convex proximally and the sutures between fore-limb elements are closed, indicative of osteological maturity, but the shaft of the humerus is textured, indicative of immaturity (Johnson 1977). Both radii are notched; this character separates embryos and small juveniles from larger juveniles in *Stenopterygius* (Johnson 1977; Maxwell et al. 2014), but is taxon-specific, with both embryos and adults of *Leptonectes*, another Early Jurassic parvipelvian ichthyosaur, showing

notched radii (Lomax and Massare 2012). The diapophyses and parapophyses are well ossified, as in large juveniles and mature individuals (Maxwell et al. 2016). In the skull, confluence between the preglenoid and paracoronoid processes is generally observed from postnatal stage 2 onwards, although some postnatal stage 1 specimens also display this feature (Miedema and Maxwell 2022). The dentary fossa is clearly defined, as is the case for postnatal stage 2 individuals (Miedema and Maxwell 2022). The posterior margin of the maxilla is composed of a single ramus, which is not the case for postnatal stage 1 specimens, but characterises postnatal 2 and adult stages (Miedema and Maxwell 2022). The lacrimal bears a moderately pronounced lateral ridge defining the anteriormost circumorbital area; this ridge is more strongly pronounced in postnatal stage 1, but less pronounced in sexually mature individuals (Miedema and Maxwell 2022). The ventral surface of the postorbital is narrower than in adult individuals, more similar to postnatal stage 1 or 2, but the bone is curved, whereas it appears straighter earlier in ontogeny (Miedema and Maxwell 2022). Finally, the position of the quadrate facet medial to the posterior bulge of the supratemporal is similar to sexually mature individuals (Miedema and Maxwell 2022). Thus, overall, postcranial, cranial and size criteria suggest an attribution to postnatal stage 2.

Generic and species determination

As the taphonomic loss of the highly diagnostic pelvic girdle prevents easy generic referral, we use a combination of characters to refer the specimen to genus. We limit comparisons to Toarcian genera, of which five are currently considered to be valid: *Temnodontosaurus*, *Eurhinosaurus*, *Suevoleviathan*, *Stenopterygius* and *Hauffiopteryx*. *Magnipterygius* Maisch & Matzke, 2022 is here considered to be a junior synonym of *Stenopterygius quadriscissus* (discussed in more detail in 'Remarks', above).

No overbite is present in SMNS 55110, unlike in *Hauffiopteryx* and *Eurhinosaurus* and the prefrontal is excluded from participation in the external nares unlike in *Hauffiopteryx* (Maxwell and Cortés 2020). Based on supratemporal morphology, the upper temporal fenestra was large and ovate to trapezoidal in shape, unlike in *Hauffiopteryx* and *Eurhinosaurus*. The degree of exposure of the angular in lateral view is only shared with the genus *Stenopterygius* (McGowan and Motani 2003; Maxwell 2012). Presacral and preflexural vertebral counts of 46 and 80, respectively in SMNS 55110 are consistent with *Stenopterygius* (44–46 presacral and 80–90 preflexural centra), *Hauffiopteryx* (46 presacral and 81 preflexural centra: Maxwell and Cortés (2020)), *Suevoleviathan* (44 presacral and 88 preflexural centra: Maisch (1998a)) and *Temnodontosaurus* (81–95 preflexural vertebrae, McGowan (1996); Swaby and Lomax (2021)), but unlike *Eurhinosaurus* (presacral count = 45–50; preflexural count 91–95, McGowan (1994); McGowan and Motani (2003)). Ribs show distinct tubercula and capitula, as in *Hauffiopteryx* and *Stenopterygius*, rather than the sheathed-bicapitate morphology observed in *Temnodontosaurus*, *Eurhinosaurus* and *Suevoleviathan.* The presence of a well-developed anterior notch on the coracoid differs from *Suevoleviathan* (Maxwell 2018). The estimation of the specimen as a large juvenile 1.46 m in total length suggests that it is most likely attributable to a taxon with an adult body size of less than 5 m total length, such as *Stenopterygius* or *Hauffiopteryx*, rather than to a large-bodied taxon such as *Temnodontosaurus*, *Suevoleviathan* or *Eurhinosaurus*. Thus, considering all cranial and postcranial characters, SMNS 55110 is entirely consistent with the genus *Stenopterygius* to the exclusion of all other Toarcian genera.

Of the three Toarcian species of *Stenopterygius* currently considered valid (*S. quadriscissus*, *S. triscissus*, *S. longipes*), *S. triscissus* is the only one to have been previously reported from the UK (Benton and Taylor 1984; Benton and Spencer 1995; Caine and Benton 2011; Lomax 2019). Based on the characters of Maisch (2008), SMNS 55110 has a prenarial ratio (0.62) more consistent with *S. quadriscissus* or small individuals of *S. longipes* (0.66) than *S. triscissus* (0.70) (Maisch 2008). We also compared measurements from our specimen with those of Maxwell (2012) for individuals with a lower jaw length of between 300 and 400 mm (Table 2). However, due to the absence of the hind-limb in SMNS 55110, comparisons were limited. Moreover, juveniles of *S. longipes* have not yet been identified, making comparisons between similar-sized individuals impossible. However, these comparisons reveal that SMNS 55110 has a fore-limb + humerus that is longer relative to the lower jaw than any specimen of *S. triscissus* in that size class.

Given how few points of comparison were possible, based on previous studies, we used the new caudal and intermedium metrics to assess the species of SMNS 55110. Caudal measurements are able to differentiate *S. quadriscissus* and *S. triscissus* (Maisch and Matzke

Table 2. Selected ratio data for *Stenopterygius* with lower jaw lengths between 300 and 400 mm (from Maxwell (2012)). Parameters for which SMNS 55110 is consistent with only one species are in bold.

	log(premaxilla)/log(lower jaw)	log(fore-limb + humerus)/ log(lower jaw)	log(fore-limb)/ log(humerus)
SMNS 55110	0.92	**0.91**	1.31
S. quadriscissus	0.89–0.91	**0.82–0.92**	1.21–1.35
S. triscissus	0.90–0.91	0.77–0.81	1.26–1.32
S. longipes	-	-	-

2022), while the intermedium measurements can differentiate all three species. SMNS 55110 has a postflexural length/total caudal length ratio of 0.42, consistent with *S. quadriscissus* (0.34–0.47), but outside the range of *S. triscissus* (0.31–0.36); 34 tailstock vertebrae, consistent with both species (*S. quadriscissus* = 33–39 vs. 34–44 for *S. triscissus*) and an intermedium Uf/Rf equal to 1.01, consistent with *S. quadriscissus*, but outside the range of both *S. triscissus* and *S. longipes* (*S. quadriscissus*: 0.54–1.07, *S. triscissus*: 1.20–1.75; *S. longipes*: 1.03–1.18).

Based on the cranial to forelimb proportions, the relatively short tailstock and the relative size of the proximal intermedium facets, SMNS 55110 is consistent with *S. quadriscissus*, but inconsistent with *S. triscissus*. The length of the humerus relative to the distal fore-limb and the relative sizes of the proximal intermedium facets provide evidence, albeit weaker than that argued above, that this specimen also cannot be assigned to *S. longipes*. Therefore, we refer SMNS 55110 to *Stenopterygius quadriscissus.*

Taphonomy

The unusually curled disposition of the axial skeleton in SMNS 55110 requires further consideration, in particular as to whether this specimen is a regurgitalite of a large predator. While the curled vertebral column of SMNS 55110 might superficially resemble that of the small *Stenopterygius* regurgitated specimen SMNS 15194 (Böttcher 1989; Serafini et al. 2025), no vertebral column torsion or breakage is present to indicate compression in a predator's gut (Fig. 9A). Moreover, there is no evidence for perimortem bone fractures or bite traces that could indicate either ingestion by a predator or evidence of scavenging, although the latter has been hypothesised to be the cause of the skeletal disarticulation observed in some marine reptiles from the Whitby Mudstone Formation (Benton and Spencer 1995). Although the carcass could have re-floated, based on the reconstructed water depth at the locality (> 30–100 m: Hallam (1997); Jarvis et al. (2024); see Reisdorf et al. (2012)), this seems unlikely based on the remarkable completeness and articulation of the distal fore-limbs and postflexural caudal skeleton.

A complex scenario is required to explain this curious body disposition. The specimen arrived at the seafloor in a more or less dorsal orientation, based on articulation of the vertebral column (Hofmann 1958; Martill 1993). However, there are indications that the skull penetrated the soft sediment first, such as posterior slumping of the dentition and anterior displacement of the circumorbital elements (in this case, the lacrimal, jugal and maxilla) (von Huene 1922; Wahl 2009; Delsett et al. 2016; Maxwell et al. 2022), although damage to the bones of the rostrum is minimal.

The skull is exposed in ventral-right lateral view, whereas the cervical centra are exposed in in dorsal-right lateral view, twisted almost 180° relative to the skull. Therefore, after landing, the specimen would have rolled on to its left side (Martill 1993). Following the onset of decay, the carcass would have partially lifted, although the rostrum remained embedded in the soft sediment serving as an anchor point and preventing re-floating. Bones from the posterior left side of the skull were thus freed from sediment and dropped to the sides. Current activity would have pushed the partially lifted postcranium towards the top of the slab, while the skull remained anchored, potentially exacerbating dislocation at the cervical-basioccipital joint and creating the curve in the vertebral column. The lateral intrusion in the soft sediment was less than the diameter of the carcass, reflected by the absence of ribs on the right side of the specimen. Another argument for the presence of a current going from the bottom of the slab towards the top is the disposition of the *Meleagrinella* valves, which are orientated with the umbo directed towards the top of the slab (= down-current) and the displacement of the isolated teeth, postfrontal and squamosal towards the top of the slab. However, the skeleton may have been subjected to additional current activity, since the displacement of the scleral ring, the supratemporal and the postorbitals to the upper left, the quadrate downward and the belemnites on the specimen plane are not entirely consistent with the proposed scenario.

The specimens of *Meleagrinella* positioned in a cluster towards the top of the slab, immediately above the vertebral column (Figs 6A, 9B), as well as rare individuals elsewhere within the circle of the skeleton appear to have settled after the carcass was present on the sea floor, based on their disposition and their absence elsewhere on the slab. *Meleagrinella* is relatively abundant in the Whitby Mudstone Formation (Caswell et al. 2009; Danise et al. 2015) and, thus, its presence is potentially unrelated to any local environmental enrichment by the ichthyosaur carcass. However, it is evident that the carcass was deposited during a period of oxic to dysoxic conditions at the sediment-water interface (Caswell et al. 2009).

Discussion

New metrics to differentiate *Stenopterygius* species

In the past, only a few ratios of cranial to postcranial elements were deemed useful for differentiating species of *Stenopterygius*. Here, for the first time, we have devised new metrics restricted to the postcranium that seemingly aid in species identification; we discuss the importance of these metrics and their reliability below.

Tail proportions and associated caudal vertebral count appear to be reliable for species differentiation in *Stenopterygius*, with *S. triscissus* never exhibiting a postflexural length/total caudal length ratio higher than 0.36, while values for *S. quadriscissus* ranged from 0.34 to 0.47. It is important to note that the highest and lowest

values pertained to juveniles (low and high values) or specimens with a tail in a poor state of preservation (low values). If these specimens are removed from the analysis, the range of values is more constrained (0.35–0.44 for *S. quadriscissus*; Fig. 3C). Therefore, even if there is a small overlap between the two species, this ratio can be a good way to help distinguish species of *Stenopterygius*.

Somewhat unsurprisingly, vertebral count is strongly correlated with the proportions of the tail. *S. quadriscissus* has a mean tailstock count lower than *S. triscissus*, consistent with caudal proportions. There is only one specimen of *S. triscissus* (out of seven if juveniles are included and five if not) with a tailstock vertebral count lower than 38 and only three *S. quadriscissus* (out of 30 if juveniles are included and 20 if juveniles and specimens with a poorly preserved tail are excluded) with a count greater than 38. GPIT-PV-30063 is the *S. triscissus* specimen with an anomalously low vertebral count. Stöhr and Werneburg (2022) indicate that the caudal vertebrae of this specimen have not been modified, making this anomaly difficult to explain other than as individual variation. However, as with caudal proportions, caudal preflexural vertebral counts seem to be a useful taxonomic tool, but should be combined with other lines of evidence.

The relative lengths of the radial and ulnar facets of the intermedium appear useful to distinguish the three Toarcian species of *Stenopterygius*. Indeed, there is no overlap in this ratio between *S. quadriscissus* and *S. triscissus* (Fig. 4B). This ratio in *S. longipes* also seems able to differentiate this species from the others, showing no overlap with *S. triscissus*. The value for only one specimen of *S. longipes* overlaps with two *S. quadriscissus* specimens, out of only three *S. quadriscissus* individuals with an ulnar facet slightly longer than the radial facet of the intermedium. The relative length of the ulnar and radial facets of the intermedium seems to be a strong character to differentiate *S. quadriscissus* from *S. triscissus* and also to differentiate *S. triscissus* from *S. longipes*; however, caution must be used when using this character to differentiate *S. quadriscissus* and *S. longipes*. We also assessed the angle between these proximal intermedium facets; however, while this is more acute in *S. quadriscissus* than in the other species, it is too variable to be used as an identification criterion.

Re-evaluation of *Stenopterygius* species distribution

The determination of SMNS 55110 as *Stenopterygius quadriscissus* makes this specimen the first definitive example of *S. quadriscissus* found in England, since previous referrals of material to this species were tentative and inconclusive (summarised by Lomax (2019); see, for example, McGowan and Motani (2003)). It therefore extends the palaeobiogeographic range of *Stenopterygius quadriscissus* considerably and demonstrates that this ichthyosaur was present in the Cleveland Basin during the Early Jurassic. It also reinforces the occurrence of *S. quadriscissus* in the Bifrons Zone; previously, only one juvenile individual (SMNS 56860) was reported from the Wilderschiefer (εIII; Bifrons Zone, ?Fibulatum Subzone) of the Posidonienschiefer Formation (Maxwell and Vincent 2016).

Few specimens have been assigned to *S. quadriscissus* outside of south-western Germany. Within Germany, *Stenopterygius quadriscissus* was described by Maisch and Ansorge (2004) from the Serpentinum Zone of the Green Series clay near Dobbertin, Mecklenburg-Vorpommern. The specimen is composed of a partial skull, preserved in three-dimensions. The specimen shows no characters diagnostic at the species level and, therefore, we revise this specimen from *S. quadriscissus* to *Stenopterygius* sp.

Two specimens of *Stenopterygius* from Luxembourg have also been referred to *Stenopterygius quadriscissus* (Godefroit 1994: MNHNL M1 and WAT 3; now NMNHL TU 664 and NMNHL TV 211). NMNHL TU 664 and TV 211 both originate from the Schistes de Grandcourt, from Schouweiler and Dudelange, respectively (Serpentinum Zone, Early Toarcian: Maubeuge and Delsate (1997)). NMNHL TU 664 is a largely complete specimen; the skull and postcranium remain in articulation, but most of the pectoral girdle and fore-limbs are missing, the pelvic girdle and hind-limbs are totally absent. The vertebral column is lost anterior to the tail bend. Despite this specimen being quite well preserved, it is indeterminate at the species level. Specimen NMNHL TV 211 preserves the skull (except for the anterior part of the snout, which is broken), right proximal fore-limb and right anterior dorsal region. The absence of a femur and the break of the snout do not permit confident assignment to species using classical methods (Maxwell 2012); however, the intermedium is well preserved, giving a Uf/Rf ratio 0.759, consistent with its determination as *Stenopterygius quadriscissus* and confirming the presence of this species in Luxembourg. This determination conflicts with the recent result obtained by Fischer et al. (2025), who identified this specimen as *S. triscissus*; an identification primarily based on the relative height of the maxilla at the mid-naris, as well as the participation of the maxilla in the anterior nares (Godefroit 1994). These characters are subject to taphonomic modifications (see results pertaining to *Magnipterygius*), with participation of the maxilla in the nares variably occurring in all three species (Maxwell 2012).

The last specimen formerly and tentatively assigned to *S. quadriscissus* (McGowan and Motani 2003; Weedon and Chapman 2022) is from Kettleness, near Whitby (WHITM SIM 876S), but later revised as *Stenopterygius* sp. due to a lack of readily identifiable features (Lomax 2019). However, the left fore-limb preserves the radial facet of the intermedium, which is longer than the ulnar facet and, therefore, supports referral of this specimen to *S. quadriscissus*, based on our new characters for differentiating species. Thus, the Ravenscar specimen and

WHITM SIM 876S are the only two examples that can be confidently identified as *S. quadriscissus* from the Toarcian of Yorkshire, at least for now.

We also re-evaluated specimens assigned to the genus *Stenopterygius* for which the species could not previously be determined. Within Germany, Theodori (1854) described a skull from Banz, Bavaria, Germany, referred to '*Ichthyosaurus*' *tenuirostris* and later assigned to '*Ichthyosaurus*' *acutirostris* by Fraas (1891). The specimen can be referred to *Stenopterygius* sp., but a determination at the species level is not possible.

In Switzerland, NMBE5014842, from the Serpentinum Zone of the Soladier Member, Staldengraben Formation, Teysachaux (von Huene 1939; Klug et al. 2024), was originally referred to *Stenopterygius longifrons* (= *Stenopterygius triscissus*: Maisch (2008)). NMBE5014842 was later deemed too poorly preserved to be referred to species (Maisch 2008); however, it has a well-preserved proximal fore-limb. The ulnar to radial facet ratio of the intermedium is 1.31, consistent only with *Stenopterygius triscissus*. We therefore consider this specimen referable to *Stenopterygius triscissus*, confirming the occurrence of this species in Switzerland.

A highly fragmented and incomplete specimen (ZIN PH 2/211) from Markha River, eastern Siberia, preserving a partial articulated vertebral column, skull fragment, femur and partial coracoid, was described as the easternmost occurrence of *Stenopterygius* sp. (Zverkov et al. 2020). While consistent with *Stenopterygius*, the preserved elements are not sufficient to refer this specimen to genus.

From France, specimens referred to *Stenopterygius* are known from the Argiles à Poissons, Curcy-sur-Orne, Calvados (early Toarcian, Serpentinum Zone: see summary in Cooper (2023)). These include NHMUK PV OR 33157/ PV OR 32685 (holotype of *S. longifrons* (Owen, 1881), including the skull, vertebral column, ribs and fore-limb; see Brignon (2018)) and two partial skulls referred to *S. triscissus*: NHMUK PV OR 32681 (see Brignon (2018)) and NHMUK PV OR 32682 (see Caine and Benton (2011); Brignon (2018)). *S. longifrons* (Owen 1881) was later synonymised with *S. triscissus* (Maisch 2008). The postcranial block of the *S. longifrons* holotype (NHMUK PV OR 32685; Brignon (2018): pl. 6D) has never been properly described and the posterior intermedium is covered by other elements. The two other partial Curcy-sur-Orne skulls (NHMUK PV OR 32681 and PV OR 32682) can be determined only as *Stenopterygius* sp. An additional skull from Normandy, also from the "Argiles à Poissons", was referred to '*Ichthyosaurus*' *tenuirostris* by Mazin (1988). The specimen is a 3D skull, lacking the majority of the anterior snout; some vertebrae and ribs are also preserved. The skull is referable to *Stenopterygius* sp., but identification at the species level is not possible. Thus, there are currently no ichthyosaur remains from the Toarcian of Curcy-sur-Orne that can be confidently determined at the species level.

Some specimens from Strawberry Bank, Illminster, UK referred to *Stenopterygius triscissus* (Serpentinum Zone, early Toarcian; BRLSI M1405, BRLSI M1407, BRLSI M1408 and BRLSI M1409) determined by Caine and Benton (2011) also require re-evaluation, since species determination of juvenile individuals was not well established at the time. BRLSI M1405, a partial specimen exposing some caudal vertebrae, dorsal ribs, pelvic girdle elements and a femur, can only be referred to *Stenopterygius* sp. BRLSI M1407, comprising a pelvic girdle and some fore-limb elements, is equally non-diagnostic at the species level. BRLSI M1408, an articulated specimen missing most of the caudal region (Caine and Benton 2011), lacks fore-limbs, pelvic girdle and the anteriormost part of the snout and, thus, also can only be referred to *Stenopterygius* sp. BRLSI M1409, also an articulated skeleton, lacks most of the snout, distal fore-limbs and hind-limbs, as well as the caudal region. Measurements of intermedium proximal articular facets indicate a longer contact with the radius than with the ulna, which is diagnostic of *Stenopterygius quadriscissus* to the exclusion of other *Stenopterygius* species. Another partial specimen (BRLSI M3558) from Strawberry Bank, UK, exposing the skull (except the distal part of the snout), both fore-limbs, ribs, vertebrae and some elements of the pectoral and pelvic girdle (damage and partial ischiopubis) was revised by Srdic et al. (2021) as *S. triscissus*. Measurements of intermedium proximal articular facets indicate a longer contact with radius than with the ulna, which is diagnostic of *Stenopterygius quadriscissus* and excludes the other *Stenopterygius* species. The material described by Srdic et al. (2021) can, therefore, be definitively attributed to *S. quadriscissus*. To sum up, *Stenopterygius quadriscissus* is present in the UK from at least the Serpentinum Zone, Exaratum Subzone (Williams et al. 2015), but there is no evidence for *S. triscissus* at the Strawberry Bank locality.

In summary, we can confirm that the palaeobiogeographic range of *Stenopterygius quadriscissus* extended from south-western Germany to the Cleveland Basin (Yorkshire), including Luxembourg and the Wessex Basin (Strawberry Bank). We can also confirm that its stratigraphic range extended from the Tenuicostatum to Bifrons Zones (Maxwell and Vincent 2016), Commune Subzone (SMNS 55110, current study). Thus, the stratigraphic range of *S. quadriscissus* is estimated to have been 3.3 +/- 0.6 Myr (calculated from Ruebsam et al. (2023); Jarvis et al. (2024)).

Distribution of ichthyosaur species during the Early Toarcian

By comparing the Toarcian ichthyosaurs from the Whitby Mudstone Formation (*Temnodontosaurus crassimanus*, *T. zetlandicus*, *T. trigonodon*?, *Stenopterygius quadriscissus*, *Eurhinosaurus longirostris*: Tate and Black (1876); Benton and Taylor (1984); Benton and Spencer (1995); Lomax (2019); Swaby and Lomax (2021); Laboury et al. (2022); Larkin et al. (2023); present study)

with the species found in the southwest German Basin (*S. quadriscissus*, *S. triscissus*, *S. longipes*, *Suevoleviathan integer*, *Hauffiopteryx typicus*, *H. altera*, *T. trigonodon*, *E. longirostris*: McGowan (1994); Maisch (1998b, 2008); Maxwell (2018); Maxwell and Cortés (2020)), it appears that, at the generic level, there are two differences, namely the presence of genera *Suevoleviathan* and *Hauffiopteryx* in the southwest German Basin, but not the Yorkshire Basin (Table 3). However, at minimum, *Hauffiopteryx typicus* is known to have been present in the Toarcian of the UK at the Strawberry Bank locality (Wessex Basin) and likely *H. altera* was as well (*H. typicus*: Caine and Benton (2011); *H. altera*: BRLSI M 1401). At the species level, the differences are slightly more significant: in southwestern Germany, there is no evidence for *T. zetlandicus* or *T. crassimanus*, while in Yorkshire (or elsewhere in the UK), there is no evidence for *S. longipes* or *S. triscissus*. The most fossiliferous horizons from the southwest German Basin are from the Tenuicostatum–Serpentinum Zones, whereas in Whitby, these are somewhat younger (Serpentinum–Bifrons Zones).

The underlying reason for the difference in diversity between the Whitby Mudstone and Posidonienschiefer Formations is likely a consequence of geological exposure and human economic activity, combined with a distinct lack of detailed assessment of the Yorkshire Lias ichthyosaurs; again, this is in part due to often poorly preserved or poorly prepared material. Most of the ichthyosaurs excavated from the Holzmaden Region originate from the Tenuicostatum Zone, historically quarried for ornamental stone (Maxwell and Vincent 2016), whereas most of the ichthyosaurs from the Whitby Mudstone Formation originated from the Alum Shale Member (Bifrons Zone), historically mined for alum (Benton and Spencer 1995), but which are still often collected from the foreshore today (Lomax 2019). The Whitby Mudstone Formation may have been deposited closer to the palaeocoastline or in a more restricted basin than the most productive southwest German localities, based on the relatively greater abundance of plesiosaurs and thalattosuchian crocodylomorphs from Whitby; these are thought to prefer nearer-shore habitats than ichthyosaurs (Godefroit 1996).

Palaeobiology and functional morphology

The greater number of tailstock vertebrae in *Stenopterygius triscissus* than *S. quadriscissus* might have functional implications for niche partitioning between these species. The number of caudal vertebrae is correlated with relative swimming speed in cetaceans (Uhen 2004), potentially due to an increase in intervertebral tissue, increasing elasticity and energy storage in the tailstock and reducing mechanical costs during swimming in a pelagic environment (Buchholtz and Gee 2017). Thus, *S. triscissus* might have faster, more efficient swimming than *S. quadriscissus*. Amongst recent odontocetes, species with higher caudal vertebral counts typically inhabit more pelagic habitats (Buchholtz and Gee 2017); this may also have applied to ichthyosaurs. Thus, the observed difference in caudal vertebral counts could support habitat segregation between *S. triscissus* and *S. quadriscissus*, with the latter possibly preferring a nearshore habitat and *S. triscissus* preferring a more pelagic environment.

A proportionately longer ulnar facet of the intermedium might result in increased width of the proximal fore-limb skeleton, which is correlated with turning speed in cetaceans (DeBlois and Motani 2019). Preliminary observations seem to support a difference in proximal limb width between *S. quadriscissus* and *S. triscissus*, supporting the hypothesis of niche partitioning between them.

Conclusions

We describe SMNS 55110, a small ichthyosaur from the Alum Shale Member of the Whitby Mudstone Formation, collected from Ravenscar near Whitby, Yorkshire, UK. During comparisons with other Toarcian species of *Stenopterygius*, we defined two new metrics (postflexural length/total caudal length and length of the ulnar facet/length of radial facet of the intermedium) that appear useful in differentiating species of this abundant genus. This comparative work resulted in the synonymisation of *S. uniter* with the senior synonym *S. longipes*

Table 3. Distribution of Early Jurassic ichthyosaurs at Yorkshire coast and southwest German Basin (von Huene 1951; Benton and Spencer 1995; Maxwell 2012, 2018; Lomax 2019; Maxwell and Cortés 2020; Swaby and Lomax 2021; Weedon and Chapman 2022; Laboury et al. 2022; Larkin et al. 2023). Abbreviations: Ten = Tenuicostatum, Serp = Serpentinum, Bif = Bifrons.

Genus	Species	Whitby Mudstone Formation			Southwest German Basin		
		Ten.	Serp.	Bif.	Ten.	Serp.	Bif.
Temnodontosaurus	*crassimanus*			X			
	zetlandicus			X			
	trigonodon		X?	X?	X	X	
Eurhinosaurus	*longirostris*		?	X	X	X	X
Stenopterygius	*quadriscissus*			X	X	X	X
	triscissus				X	X	X
	longipes					X	
Hauffiopteryx	*typicus*				X	X	
	altera					X	
Suevoleviathan	*integer*					X	X

and *Magnipterygius huenei* with the senior synonym *S. quadriscissus*. SMNS 55110 is also consistent with the species *Stenopterygius quadriscissus*, confirming the presence of this taxon in the Yorkshire Cleveland Basin (see also WHITM SIM 876S) and, on a broader scale, in the northernmost part of the European epicontinental sea. This is the first definite example of *S. quadriscissus* from the UK. SMNS 55110 reinforces the presence of *S. quadriscissus* during the Bifrons Zone, making it one of the youngest occurrences of this species. Our new anatomical criteria permitted a revision of the distribution of the most abundant *Stenopterygius* species during the Toarcian, with *S. triscissus* confirmed only in the southwest German Basin and Switzerland and absent from Strawberry Bank and *S. quadriscissus* having a much broader distribution, with confirmed occurrences in Luxembourg, southwest German Basin, Yorkshire and Strawberry Bank, UK (see Discussion). Differences in caudal morphology between the two species may reflect differences in locomotor specialisations and potentially habitat use.

Acknowledgements

Thanks to I. Werneburg (GPIT) for collections access and to H. Wright and R. Osborne (WHITM) for providing access to comparative material. S. Cooper and E. Mujal generously provided feedback on the figures. Thanks to P. Doyle for expert advice on the belemnite determinations. T. Biot was supported by the Erasmus+ programme during his stay in Stuttgart. DRL wishes to acknowledge The Royal Commission for the Exhibition of 1851 for generous support in the form of a Research Fellowship. Feedback from D. Martill and an anonymous reviewer improved this manuscript.

References

Andrews CW (1910) A descriptive catalogue of the marine reptiles of the Oxford Clay. British Museum of Natural History, London, Vol. 1, 205 pp.

Bardet N (1992) Stratigraphic evidence for the extinction of the ichthyosaurs. Terra Nova 4(6): 649–656. https://doi.org/10.1111/j.1365-3121.1992.tb00614.x

Bennion RF, Maxwell EE, Lambert O, Fischer V (2024) Craniodental ecomorphology of the large Jurassic ichthyosaurian *Temnodontosaurus*. Journal of Anatomy 244(1): 22–41. https://doi.org/10.1111/joa.13939

Benton MJ, Spencer PS (1995) Fossil Reptiles of Great Britain. Chapman and Hall, London, 355 pp. https://doi.org/10.1007/978-94-011-0519-4

Benton MJ, Taylor MA (1984) Marine reptiles from the Upper Lias (Lower Toarcian, Lower Jurassic) of the Yorkshire coast. Proceedings of the Yorkshire Geological Society 44(4): 399–429. https://doi.org/10.1144/pygs.44.4.399

Blainville HM (1835) Description de quelques espèces de reptiles de la Californie, précédé de l'analyse d'un système général d'erpétologie et d'amphibiologie. Nouvelles Annales du Muséum d'Histoire Naturelle, Paris 4: 233–296.

Böttcher R (1989) Über die Nahrung eines *Leptopterygius* (Ichthyosauria, Reptilia) aus dem süddeutschen Posidonienschiefer (Unterer Jura) mit Bemerkungen über den Magen der Ichthyosaurier. Stuttgarter Beiträge zur Naturkunde Serie B (Geologie und Paläontologie) 155: 1–19.

Brignon A (2018) La collection de vertébrés jurassiques du Calvados de Pierre Tesson. Bourg-la-Reine, Paris, 82 pp.

Buchholtz EA (2001) Swimming styles in Jurassic ichthyosaurs. Journal of Vertebrate Paleontology 21(1): 61–73. https://doi.org/10.1671/0272-4634(2001)021[0061:SSIJI]2.0.CO;2

Buchholtz EA, Gee JK (2017) Finding sacral: Developmental evolution of the axial skeleton of odontocetes (Cetacea). Evolution & Development 19(4–5): 190–204. https://doi.org/10.1111/ede.12227

Caine H, Benton MJ (2011) Ichthyosauria from the Upper Lias of Strawberry Bank, England. Palaeontology 54(5): 1069–1093. https://doi.org/10.1111/j.1475-4983.2011.01093.x

Caswell BA, Coe AL, Cohen AS (2009) New range data for marine invertebrate species across the early Toarcian (Early Jurassic) mass extinction. Journal of the Geological Society, London 166: 859–872. https://doi.org/10.1144/0016-76492008-0831

Cooper SLA (2023) Cannibalism in the Early Jurassic bony fish *Pachycormus macropterus* (Teleosteomorpha: Pachycormiformes) and its paleoecological significance. Journal of Vertebrate Paleontology 43(3): e2294000. https://doi.org/10.1080/02724634.2023.2294000

Danise S, Twitchett RJ, Little CTS (2015) Environmental controls on Jurassic marine ecosystems during global warming. Geology 43(3): 263–266. https://doi.org/10.1130/g36390.1

DeBlois MC, Motani R (2019) Flipper bone distribution reveals flexible trailing edge in underwater flying marine tetrapods. Journal of Morphology 280(6): 908–924. https://doi.org/10.1002/jmor.20992

Delsett LL, Novis LK, Roberts AJ, Koevoets MJ, Hammer Ø, Druckenmiller PS, Hurum JH (2016) The Slottsmøya marine reptile *Lagerstätte*: depositional environments, taphonomy and diagenesis. Geological Society, London, Special Publications 434(1): 165–188. https://doi.org/10.1144/SP434.2

Fischer V, Guiomar M, Godefroit P (2011) New data on the palaeobiogeography of Early Jurassic marine reptiles: the Toarcian ichthyosaur fauna of the Vocontian Basin (SE France). Neues Jahrbuch für Geologie und Palaontologie Abhandlungen 261(1): 1–12. https://doi.org/10.1127/0077-7749/2011/0155

Fischer V, Weis R, Delsate DF, Della Giustina F, Wintgens P, Fuchs D, Thuy B (2025) Vampyromorph coleoid predation by an ichthyosaurian from the Early Jurassic Lagerstätte of Bascharage, Luxembourg. PeerJ 13: e19786. https://doi.org/10.7717/peerj.19786

Fraas E (1891) Ichthyosaurier der süddeutschen Trias- und Jura- Ablagerungen. H. Laupp, Tübingen, 81 pp.

Godefroit P (1994) Les reptiles marins du Toarcien (Jurassique inférieur) belgo-luxembourgeois 39. Service géologique de Belgique.

Godefroit P (1996) Biodiversité des reptiles marins du Jurassique inférieur belgo-luxembourgeois. Bulletin de la Société belge de Géologie 104(1–2): 67–76.

Hallam A (1997) Estimates of the amount and rate of sea-level change across the Rhaetian-Hettangian and Pliensbachian–Toarcian boundaries (latest Triassic to Early Jurassic). Journal of the Geological Society 154: 773–779. https://doi.org/10.1144/gsjgs.154.5.0773

Hesselbo SP (2008) Sequence stratigraphy and inferred relative sea-level change from the onshore British Jurassic. Proceedings of the

Geologists' Association 119(1): 19–34. https://doi.org/10.1016/S0016-7878(59)80069-9

Hesselbo SP, Jenkyns HC (1999) British Lower Jurassic sequence stratigraphy. SEPM Special Publication 60: 561–583. https://doi.org/10.2110/pec.98.02.0561

Hesselbo SP, Jenkyns HC, Duarte LV, Oliveira LC (2007) Carbon-isotope record of the Early Jurassic (Toarcian) Oceanic Anoxic Event from fossil wood and marine carbonate (Lusitanian Basin, Portugal). Earth and Planetary Science Letters 253(3–4): 455–470. https://doi.org/10.1016/j.epsl.2006.11.009

Hofmann J (1958) Einbettung und Zerfall der Ichthyosaurier im Lias von Holzmaden. Meyniana 6: 10–55. https://doi.org/10.2312/meyniana.1958.6.10

Howarth MK (1962) The jet rock series and the alum shale series of the Yorkshire coast. Proceedings of the Yorkshire Geological Society 33(4): 381–422. https://doi.org/10.1144/pygs.33.4.381

Huene F (1922) Die Ichthyosaurier des Lias und ihre Zusammenhänge. Verlag von Gebrüder Borntraeger, Berlin, 114 pp.

Huene F (1931) Neue Studien über Ichthyosaurier aus Holzmaden. Abhandlungen der Senckenbergischen Naturforschenden Gesellschaft 42: 345–382.

Huene F (1939) Ein ganzes Ichthyosaurier-Skelett aus den west-schweizerischen Voralpen. Mitteilungen der Naturforschenden Gesellschaft 1939: 1–14. https://doi.org/10.5169/seals-319655

Huene F (1949) Ein Versuch, die *Stenopterygius*-Arten des Oberen Lias in Zusammenhang zu bringen. Neues Jahrbuch für Mineralogie, Geologie und Paläontologie, Monatschefte 1949: 80–88.

Huene F (1951) Ein neuer Fund von *Eurhinosaurus longirostris*. Neues Jahrbuch für Geologie und Palaeontologie, Abhandlungen 93: 277–284.

Hungerbühler A (1994) Recently identified type material of the Lower Jurassic ichthyosaur *Stenopterygius* in the Geological-Paleontological Institute, Tübingen. Paläontologische Zeitschrift 68: 245–258.

Jaekel O (1904) Die Wirbeltiere. Eine Übersicht über die fossilen und lebenden Formen. Gebrüder Borntraeger, Berlin, 252 pp. https://doi.org/10.5962/bhl.title.119340

Jarvis I, Atar E, Gröcke DR, Herringshaw LG, Trabucho-Alexandre JP (2024) A global reference for black shale geochemistry and the T-OAE revisited: upper Pliensbachian–middle Toarcian (Lower Jurassic) chemostratigraphy in the Cleveland Basin, England. Geological Magazine 161: e13. https://doi.org/10.1017/s0016756824000244

Johnson R (1977) Size independent criteria for estimating relative age and the relationship among growth parameters in a group of fossil reptiles (Reptilia: Ichthyosauria). Canadian Journal of Earth Sciences 14: 1916–1924. https://doi.org/10.1139/e77-162

Johnson R (1979) The osteology of the pectoral complex of *Stenopterygius* Jaekel Reptilia: Ichthyosauria. Neues Jahrbuch für Geologie und Palaeontologie Abhandlungen 159(1): 41–86. https://doi.org/10.1127/njgpa/159/1979/41

Johnson MM, Mujal E, Cooper SLA, Maxwell EE (2025) Criteria for inferring seafloor arrival position in teleosauroid carcasses (Crocodylomorpha: Thalattosuchia) and comparison with other marine vertebrates. Geological Magazine 162: e19. https://doi.org/10.1017/S0016756825100058

Kear BP, Engelschiøn VS, Hammer Ø, Roberts AJ, Hurum JH (2023) Earliest Triassic ichthyosaur fossils push back oceanic reptile origins. Current Biology 33(5): R178–R179. https://doi.org/10.1016/j.cub.2022.12.053

Kemp DB, Suan G, Fantasia A, Jin S, Chen W (2022) Global organic carbon burial during the Toarcian oceanic anoxic event: Patterns and controls. Earth-Science Reviews 231: 104086. https://doi.org/10.1016/j.earscirev.2022.104086

Klug C, Sivgin T, Miedema F, Scheffold B, Reisdorf AG, Stössel I, Maxwell EE, Scheyer TM (2024) Swiss ichthyosaurs – a review. Swiss Journal of Palaeontology 143: 31. https://doi.org/10.1186/s13358-024-00327-4

Krencker FN, Lindström S, Bodin S (2019) A major sea-level drop briefly precedes the Toarcian oceanic anoxic event: implication for Early Jurassic climate and carbon cycle. Scientific Reports 9(1): 12518. https://doi.org/10.1038/s41598-019-48956-x

Laboury A, Bennion RF, Thuy B, Weis R, Fischer V (2022) Anatomy and phylogenetic relationships of *Temnodontosaurus zetlandicus* (Reptilia: Ichthyosauria). Zoological Journal of the Linnean Society 195(1): 172–194. https://doi.org/10.1093/zoolinnean/zlab118

Larkin NR, Lomax DR, Evans M, Nicholls E, Dey S, Boomer I, Davis J (2023) Excavating the 'Rutland Sea Dragon': The largest ichthyosaur skeleton ever found in the UK (*Temnodontosaurus*, Whitby Mudstone Formation, Toarcian, Lower Jurassic). Proceedings of the Geologists' Association 134(5–6): 627–640. https://doi.org/10.1016/j.pgeola.2023.09.003

Lomax DR, Massare JA (2012) The first reported *Leptonectes* (Reptilia: Ichthyosauria) with associated embryos, from Somerset, England. Paludicola 8: 263–276.

Lomax DR, Gibson BJ (2015) The first definitive occurrence of *Ichthyosaurus* and *Temnodontosaurus* (Reptilia: Ichthyosauria) in Nottinghamshire, England and a review of ichthyosaur specimens from the county. Proceedings of the Geologists' Association 126(4–5): 554–563. https://doi.org/10.1016/j.pgeola.2015.05.006

Lomax DR (2019) Ichthyopterygia. In: Lord AR, Munt M (Eds) Fossils from the Lias of the Yorkshire Coast. The Palaeontological Association 317–331.

Lomax DR, Massare JA, Evans M (2020) New information on the skull roof of *Protoichthyosaurus* (Reptilia: Ichthyosauria) and intraspecific variation in some dermal skull elements. Geological Magazine 157(4): 640–650. https://doi.org/10.1017/s0016756819001225

Maisch MW (1998a) Kurze Übersicht der Ichthyosaurier des Posidonienschiefers mit Bemerkungen zur Taxonomie der Stenopterygiidae und Temnodontosauridae. Neues Jahrbuch für Geologie und Palaontologie Abhandlungen 209(3): 401–431.

Maisch MW (1998b) A new ichthyosaur genus from the Posidonia Shale (Lower Toarcian, Jurassic) of Holzmaden, SW-Germany with comments on the phylogeny of post-Triassic ichthyosaurs. Neues Jahrbuch für Geologie und Paläontologie Abhandlungen 209(1): 47–78. https://doi.org/10.1127/njgpa/209/1998/47

Maisch MW (2008) Revision der Gattung *Stenopterygius* Jaekel, 1904 emend. von Huene, 1922 (Reptilia: Ichthyosauria) aus dem unteren Jura Westeuropas. Palaeodiversity 1: 227–271.

Maisch MW, Ansorge J (2004) The Liassic ichthyosaur *Stenopterygius* cf. *quadriscissus* from the lower Toarcian of Dobbertin (northeastern Germany) and some considerations on lower Toarcian marine reptile palaeobiogeography. Paläontologische Zeitschrift 78: 161–171. https://doi.org/10.1007/bf03009136

Maisch MW, Matzke AT (2022) *Magnipterygius huenei* n. gen. n. sp., a new small stenopterygiid (Reptilia: Ichthyosauria) from the Posidonienschiefer Formation of SW Germany. Neues Jahrbuch für Geologie und Paläontologie-Abhandlungen 303(2): 169–201. https://doi.org/10.1127/njgpa/2022/1042

Marek RD, Moon BC, Williams M, Benton MJ (2015) The skull and endocranium of a Lower Jurassic ichthyosaur based on digital reconstructions. Palaeontology 58(4): 723–742. https://doi.org/10.1111/pala.12174

Martill DM (1993) Soupy substrates: a medium for the exceptional preservation of ichthyosaurs of the Posidonia Shale (Lower Jurassic) of Germany. Kaupia 2: 77–97.

Martin JE, Suan G, Suchéras-Marx B, Rulleau L, Schlögl J, Janneau K, Williams M, Léna A, Grosjean A-S, Sarroca E, Perrier V, Fernandez V, Charruault A-L, Maxwell EE, Vincent P (2021) Stenopterygiids from the lower Toarcian of Beaujolais and a chemostratigraphic context for ichthyosaur preservation during the Toarcian Oceanic Anoxic Event. Geological Society, London, Special Publications 514: 153–172. https://doi.org/10.1144/sp514-2020-232

Massare JA, Lomax DR (2018) A taxonomic reassessment of *Ichthyosaurus communis* and *I. intermedius* and a revised diagnosis for the genus. Journal of Systematic Palaeontology 16(3): 263–277. https://doi.org/10.1080/14772019.2017.1291116

Maubeuge PL, Delsate D (1997) Notes paléontologiques et biostratigraphiques sur le Grand Duché de Luxembourg et les régions voisines. Travaux scientifiques du MNHN Tome 27.

Maxwell EE (2012) New metrics to differentiate species of *Stenopterygius* (Reptilia: Ichthyosauria) from the Lower Jurassic of southwestern Germany. Journal of Paleontology 86(1): 105–115. https://doi.org/10.1666/11-038.1

Maxwell EE (2018) Redescription of the 'lost' holotype of *Suevoleviathan integer* (Bronn, 1844) (Reptilia: Ichthyosauria). Journal of Vertebrate Paleontology 38(2): e1439833. https://doi.org/10.1080/02724634.2018.1439833

Maxwell EE, Vincent P (2016) Effects of the early Toarcian Oceanic Anoxic Event on ichthyosaur body size and faunal composition in the Southwest German Basin. Paleobiology 42(1): 117–126. https://doi.org/10.1017/pab.2015.34

Maxwell EE, Cortés D (2020) A revision of the Early Jurassic ichthyosaur *Hauffiopteryx* (Reptilia: Ichthyosauria), and description of a new species from southwestern Germany. Papers in Palaeontology 6(4): e1390. https://doi.org/10.26879/937

Maxwell EE, Fernández MS, Schoch RR (2012) First diagnostic marine reptile remains from the Aalenian (Middle Jurassic): a new ichthyosaur from southwestern Germany. PLoS ONE 7:e41692. https://doi.org/10.1371/journal.pone.0041692

Maxwell EE, Scheyer TM, Fowler DA (2014) An evolutionary and developmental perspective on the loss of regionalization in the limbs of derived ichthyosaurs. Geological Magazine 151(1): 29–40. https://doi.org/10.1017/s0016756812001070

Maxwell EE, Dick D, Padilla S, Parra ML (2016) A new ophthalmosaurid ichthyosaur from the Early Cretaceous of Colombia. Papers in Palaeontology 2(1): 59–70.

Maxwell EE, Cooper SL, Mujal E, Miedema F, Serafini G, Schweigert G (2022) Evaluating the existence of vertebrate deadfall communities from the Early Jurassic Posidonienschiefer Formation. Geosciences 12(4): 158. https://doi.org/10.3390/geosciences12040158

Mazin J-M (1988) Le crâne d'*Ichthyosaurus tenuirostris* Conybeare, 1822 (Toarcien, La Caîne, Normandie, France). Bulletin de la Société Linnéenne de Normandie 112–113: 121–132.

McGowan C (1976) The description and phenetic relationships of a new ichthyosaur genus from the Upper Jurassic of England. Canadian Journal of Earth Sciences 13: 668–683. https://doi.org/10.1139/e76-070

McGowan C (1979) A revision of the Lower Jurassic ichthyosaurs of Germany with the description of two new species. Palaeontographica, Abteilung A 166: 93–135.

McGowan C (1989) Computed tomography reveals further details of *Excalibosaurus*, a putative ancestor for the swordfish-like ichthyosaur *Eurhinosaurus*. Journal of Vertebrate Paleontology 9(3): 269–281. https://doi.org/10.1080/02724634.1989.10011762

McGowan C (1994) The taxonomic status of the Upper Liassic ichthyosaur *Eurhinosaurus longirostris*. Palaeontology 37(4): 747–754. https://doi.org/10.5281/zenodo.16391606

McGowan C, Motani R (2003) Ichthyopterygia. Handbook of Paleoherpetology, Part 8. Verlag Dr. Friedrich Pfeil, Munich, Germany, 175 pp.

Miedema F, Maxwell EE (2022) Ontogenetic variation in the skull of *Stenopterygius quadriscissus* with an emphasis on prenatal development. Scientific Reports 12(1): 1707. https://doi.org/10.1038/s41598-022-05540-0

Miedema F, Maxwell EE (2019) Ontogeny of the braincase in *Stenopterygius* (Reptilia, Ichthyosauria) from the Lower Jurassic of Germany. Journal of Vertebrate Paleontology 39(4): e1675164. https://doi.org/10.1080/02724634.2019.1675164

Moon BC, Kirton AM (2016) Ichthyosaurs of the British Middle and Upper Jurassic Part 1, *Ophthalmosaurus*. Monographs of the Palaeontographical Society 170(647): 1–84. https://doi.org/10.1080/02693445.2016.11963958

Motani R (1999) Phylogeny of the Ichthyopterygia. Journal of Vertebrate Paleontology 19(3): 473–496. https://doi.org/10.1080/02724634.1999.10011160

Motani R (2005) Evolution of fish-shaped reptiles (Reptilia: Ichthyopterygia) in their physical environments and constraints. Annual Review of Earth and Planetary Sciences 33(1): 395–420. https://doi.org/10.1146/annurev.earth.33.092203.122707

Owen R (1881) A Monograph of the Fossil Reptilia of the Liassic Formations. Part Third. Ichthyopterygia. Palaeontographical Society, London 83–134. https://doi.org/10.1080/02693445.1881.12027969

Pardo-Pérez J, Kear BP, Maxwell EE (2019) Palaeoepidemiology in extinct vertebrate populations: factors influencing skeletal health in Jurassic marine reptiles. Royal Society Open Science 6: 190264. https://doi.org/10.1098/rsos.190264

Quenstedt FA (1856–1858) Der Jura. H. Laupp, Tübingen, 842 pp.

Reisdorf AG, Bux R, Wyler D, Benecke M, Klug C, Maisch MW, Wetzel A (2012) Float, explode or sink: postmortem fate of lung-breathing marine vertebrates. Palaeobiodiversity and Palaeoenvironments 92: 67–81. https://doi.org/10.1007/s12549-011-0067-z

Roberts AJ, Rucinski M, Kear BP, Hammer Ø, Engelschiøn VS, Scharling TH, Larsen RB, Hurum JH (2025) Earliest oceanic tetrapod ecosystem reveals rapid complexification of Triassic marine communities. Science 390(6774): 722–727. https://doi.org/10.1126/science.adx7390

Rosales I, Quesada S, Robles S (2004) Paleotemperature variations of Early Jurassic seawater recorded in geochemical trends of belemnites from the Basque–Cantabrian basin, northern Spain. Palaeogeography, Palaeoclimatology, Palaeoecology 203(3–4): 253–275. https://doi.org/10.1016/s0031-0182(03)00686-2

Ruebsam W, Schmid-Röhl A, Al-Husseini M (2023) Astronomical timescale for the early Toarcian (Early Jurassic) Posidonia Shale and global environmental changes. Palaeogeography,

Palaeoclimatology, Palaeoecology 623: 111619. https://doi.org/10.1016/j.palaeo.2023.111619

Sander PM (2000) Ichthyosauria: their diversity, distribution, and phylogeny. Paläontologische Zeitschrift 74: 1–35. https://doi.org/10.1007/bf02987949

Sander PM, Griebeler EM, Klein N, Juarbe JV, Wintrich T, Revell LJ, Schmitz L (2021) Early giant reveals faster evolution of large body size in ichthyosaurs than in cetaceans. Science 374(6575): eabf5787. https://doi.org/10.1126/science.abf5787

Serafini G, Miedema F, Schweigert G, Maxwell EE (2025) *Temnodontosaurus* bromalites from the Lower Jurassic of Germany: hunting, digestive taphonomy and prey preferences in a macropredatory ichthyosaur. Papers in Palaeontology 11(3): e70018. https://doi.org/10.1002/spp2.70018

Sharpe T (2024) The Early Jurassic sequence of Lyme Regis, Dorset, England and its place in the history of geology and palaeontology. Geological Society, London, Special Publications 543: 253–266. https://doi.org/10.1144/sp543-2023-42

Simms MJ (2004) The Cleveland Basin. In: Simms MJ, Chidlaw N, Morton N, Page KN (Eds) British Lower Jurassic Stratigraphy, Geological Conservation Review Series No. 30. Joint Nature Conservation Committee, Peterborough, 239–304.

Srdic A, Beardmore S, Lomax DR (2021) A rediscovered Lower Jurassic ichthyosaur skeleton possibly from the Strawberry Bank Lagerstätte, Somerset, UK, Historical Biology, 814–822. https://doi.org/10.1080/08912963.2019.1663840

Stöhr H, Werneburg I (2022) The Tübingen collection of ichthyosaurs from the Lower Jurassic (Lower Toarcian) Posidonienschiefer Formation of Württemberg: a historical and curatorial perspective. Palaeodiversity 16(1): 39–97. https://doi.org/10.18476/pale.v16.a3

Suan G, Mattioli E, Pittet B, Mailliot S, Lécuyer C (2008) Evidence for major environmental perturbation prior to and during the Toarcian (Early Jurassic) oceanic anoxic event from the Lusitanian Basin, Portugal. Paleoceanography 23(1): PA1202. https://doi.org/10.1029/2007PA001459

Swaby EJ, Lomax DR (2021) A revision of *Temnodontosaurus crassimanus* (Reptilia: Ichthyosauria) from the Lower Jurassic (Toarcian) of Whitby, Yorkshire, UK. Historical Biology 33(11): 2715–2731. https://doi.org/10.1080/08912963.2020.1826469

Tate R, Blake JF (1876) The Yorkshire Lias. John Van Voorst, London, 475 pp.

Theodori CV (1854) Beschreibung des kolossalen *Ichthyosaurus trigonodon* in der Lokal-Petrefakten-Sammlung zu Banz. Franz, Munich, 81 pp.

Uhen MD (2004) Form, function, and anatomy of *Dorudon atrox* (Mammalia, Cetacea): an archaeocete from the middle to late Eocene of Egypt. University of Michigan, Ann Arbor, 238 pp.

Wahl WR (2009) Taphonomy of a nose dive: bone and tooth displacement and mineral accretion in an ichthyosaur skull. Paludicola 7: 107–116.

Weedon GP, Chapman SD (2022) Ichthyosaurs from the Early Jurassic of Britain. Siri Scientific Press.

Williams M, Benton MJ, Ross A (2015) The Strawberry Bank Lagerstätte reveals insights into Early Jurassic life. Journal of the Geological Society 172(6): 683–692. https://doi.org/10.1144/jgs2014-144

Wurstemberger ARC (1876) Ueber Lias Epsilon. Jahreshefte des Vereins für vaterländische Naturkunde in Württemberg 32: 193–233.

Zverkov N, Grigoriev DV, Danilov IG (2020) Early Jurassic palaeopolar marine reptiles of Siberia. Geological Magazine 158(7): 1305–1322. https://doi.org/10.1017/s0016756820001351